Glasses in the light of X-rays

> Glass transition

> Poor mans introduction to MCT

> Dynamics with synchrotron radiation

> Metallic glasses

> Structure determination

> Stress strain properties

Hermann Franz

Research course on disordered systems

19 February 2010

HELMHOLTZ GEMEINSCHAFT

DESY

Introduction

Physical properties change gradually on lowering the temperature

Cross-over depends on cooling/heating rate

i.e. properties depend on thermal history

Glasses are in a frozen in metastable state

►susceptible to crystallisation

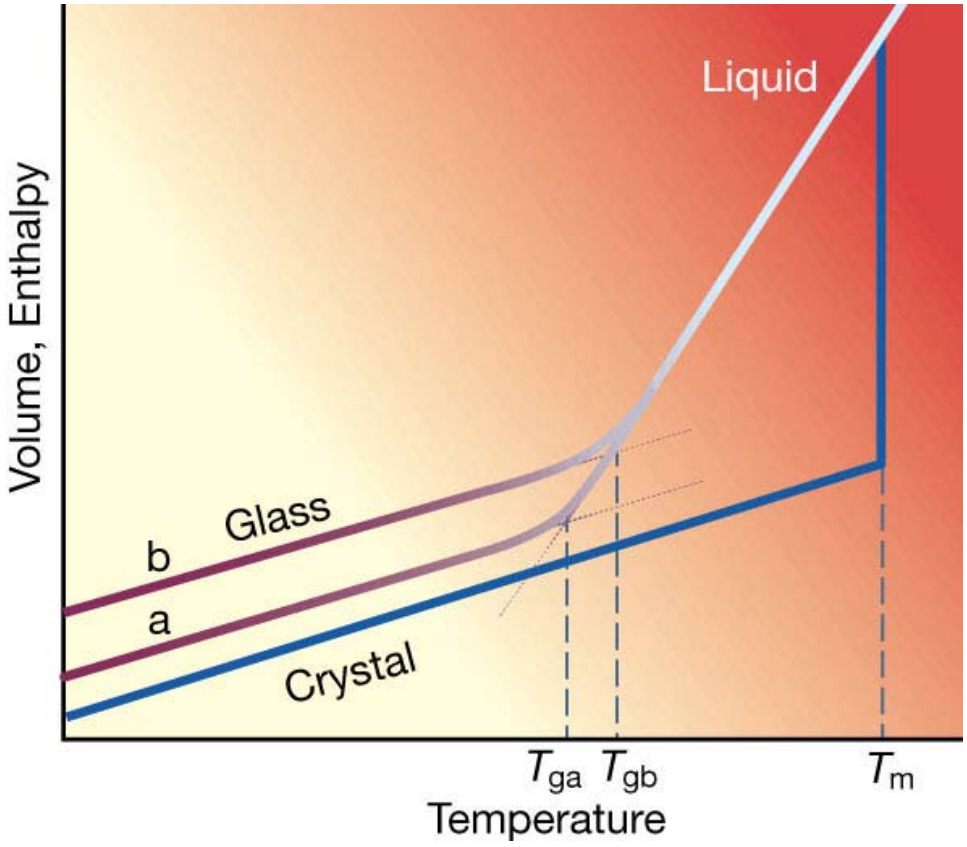

The glass transition temperature T_g

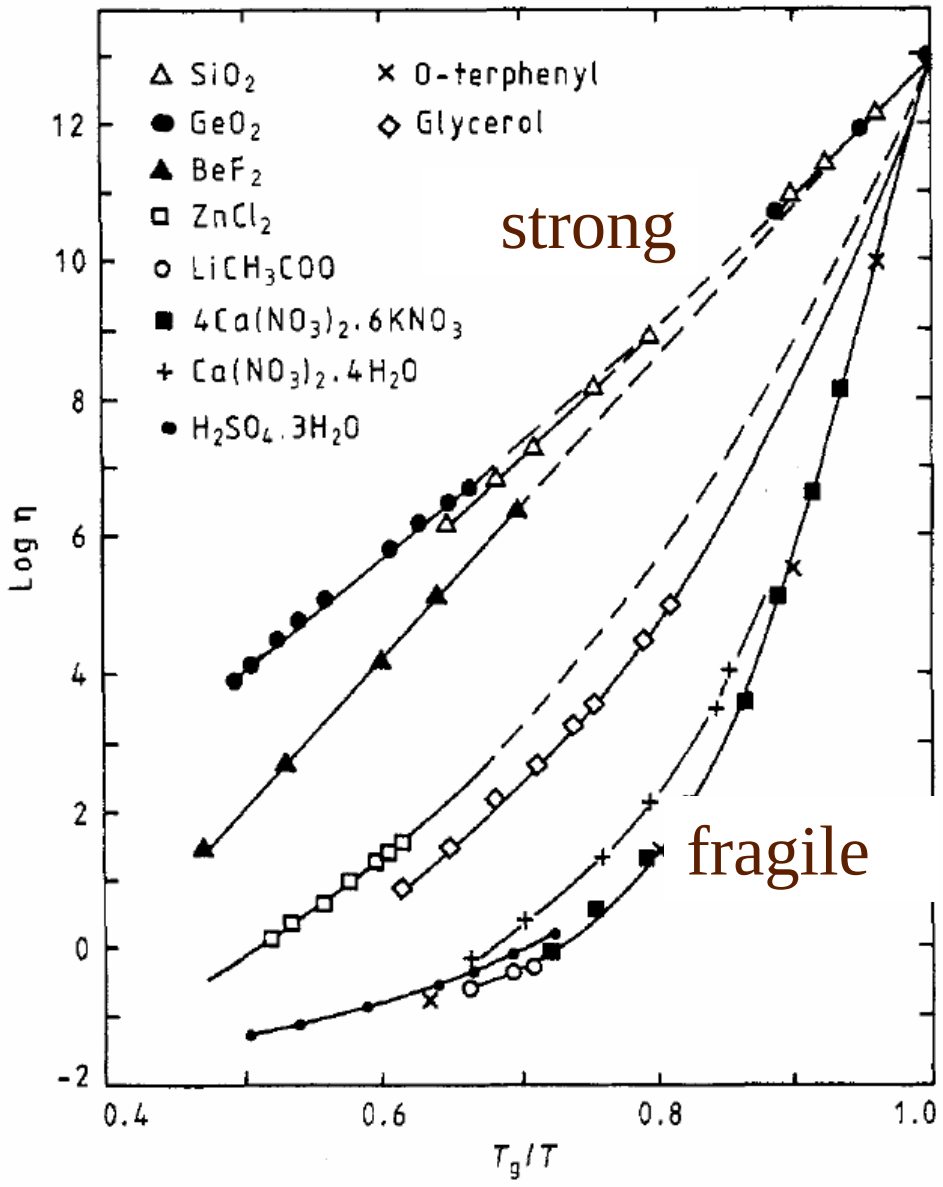

$$\eta = \exp\left(-\frac{E_0}{k(T - T_0)}\right)$$

VFT law

transition temperature T_0

Very strong variation of η / τ with temperature

T_g determined by state of the experimental technique

Structure by X-rays temperature dependence

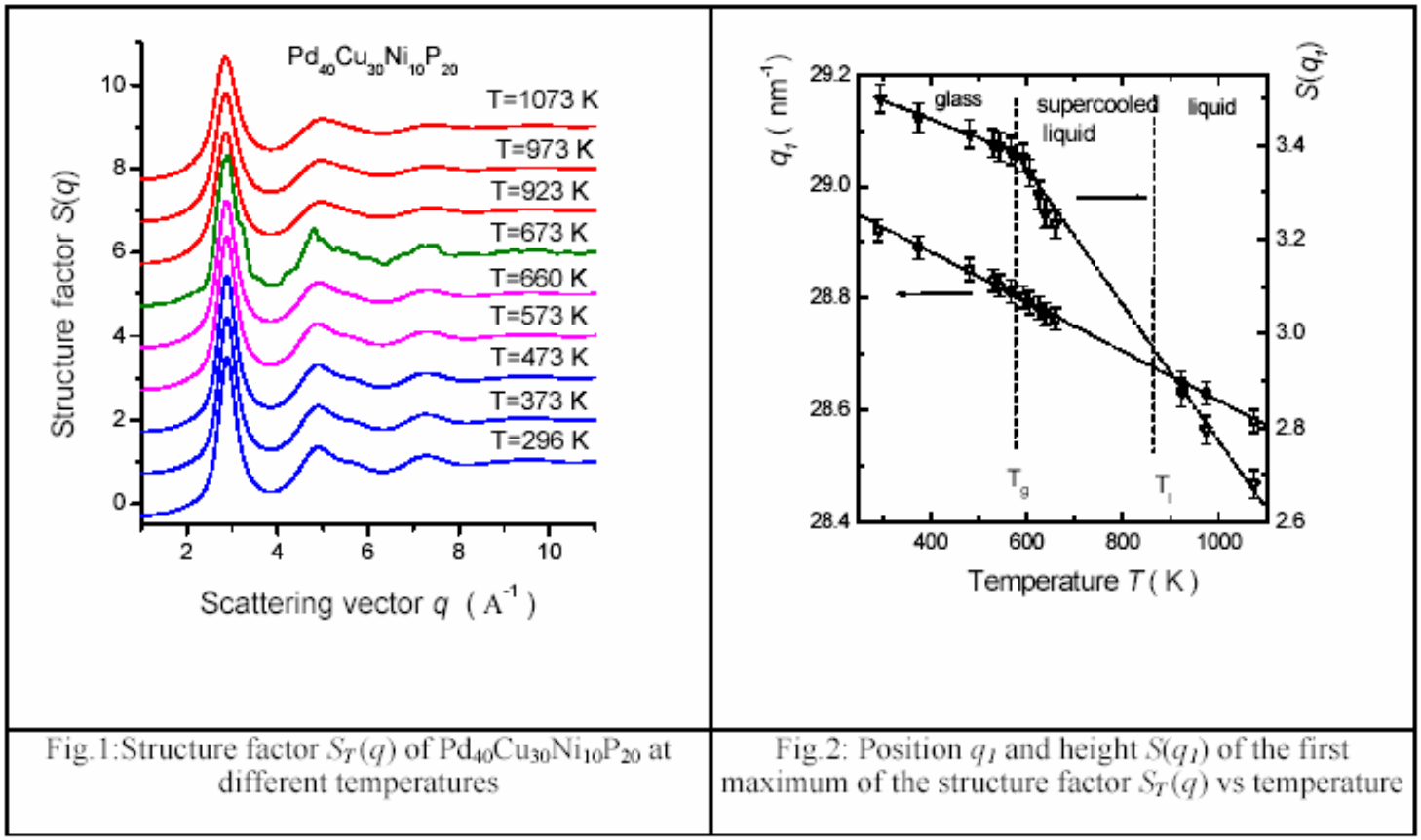

Fig.1:Structure factor $S_T(q)$ of $Pd_{40}Cu_{30}Ni_{10}P_{20}$ at different temperatures

Fig.2: Position q_1 and height $S(q_1)$ of the first maximum of the structure factor $S_T(q)$ vs temperature

N. Mattern et al

APL 2003

Below T_g: harmonic change, described by Debye behavior

At T_g: Transition to lower Debye-temperature

+ structural changes

Differential Scanning Calorimetry (DSC)

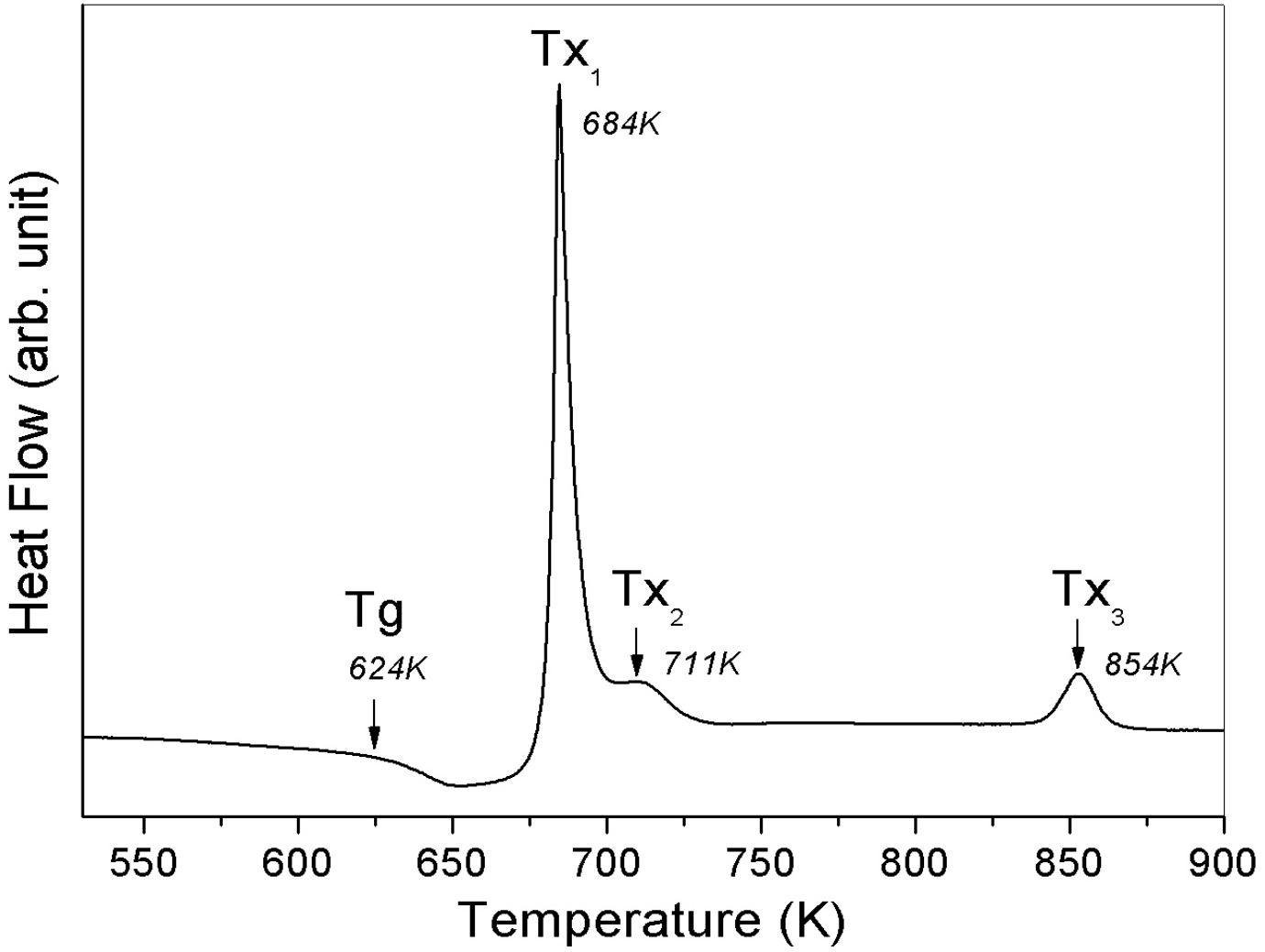

Differential Scanning Calorimetry

Supercooled liquid region:

$$\Delta T = T_{onsetx} - T_g$$

Glass forming ability (GFA)

$$\Delta T$$

$$T_{rg} = T_g / T_m$$

and many others

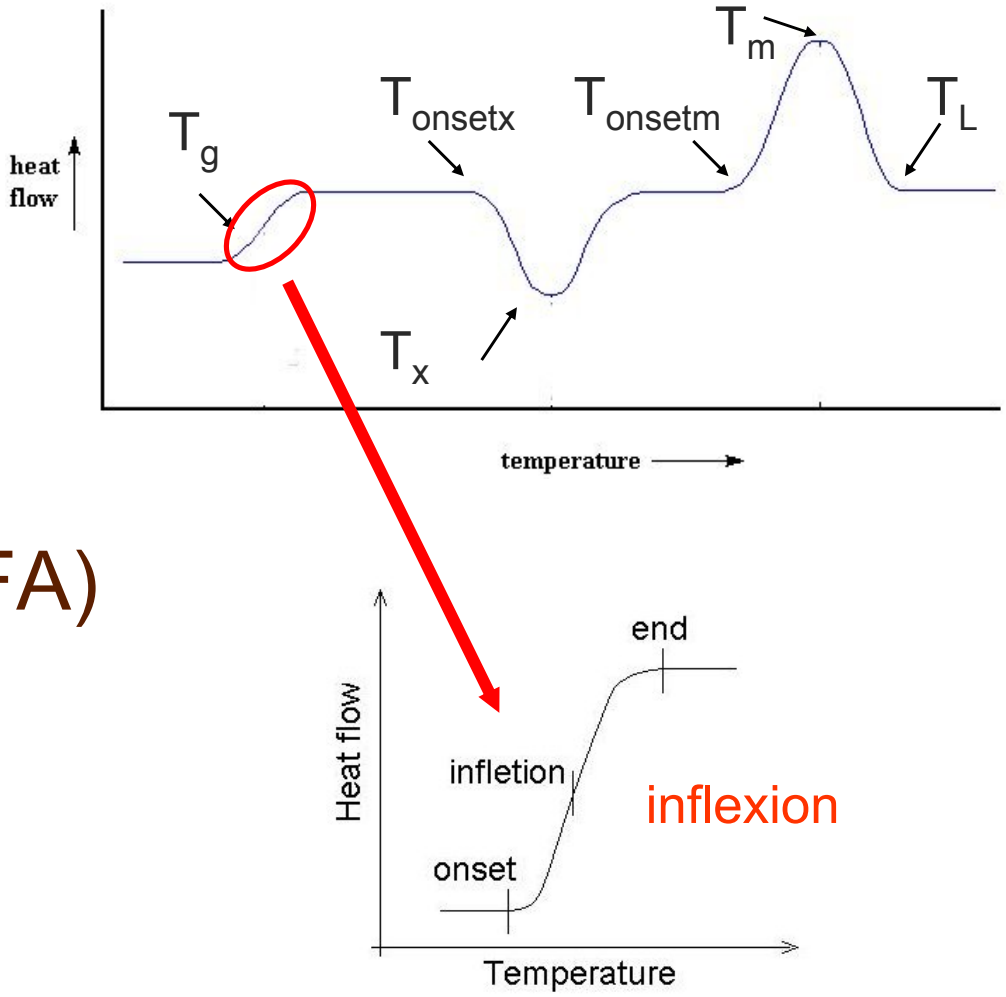

Dynamics in disordered solids

- microscopic process: rather harmonic in most glasses

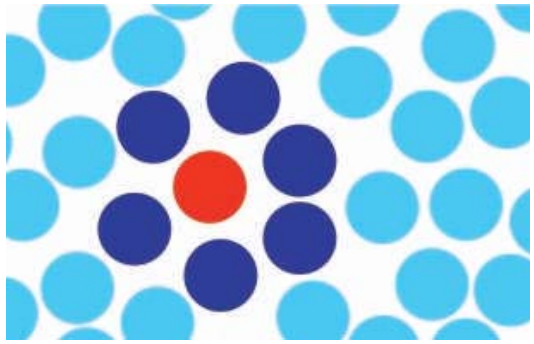

- cage (β)- process: intermediate times

α- process: long range diffusion, very strong T-dependence, stretched exponential $f_q \exp(-(t/\tau)^{\beta})$

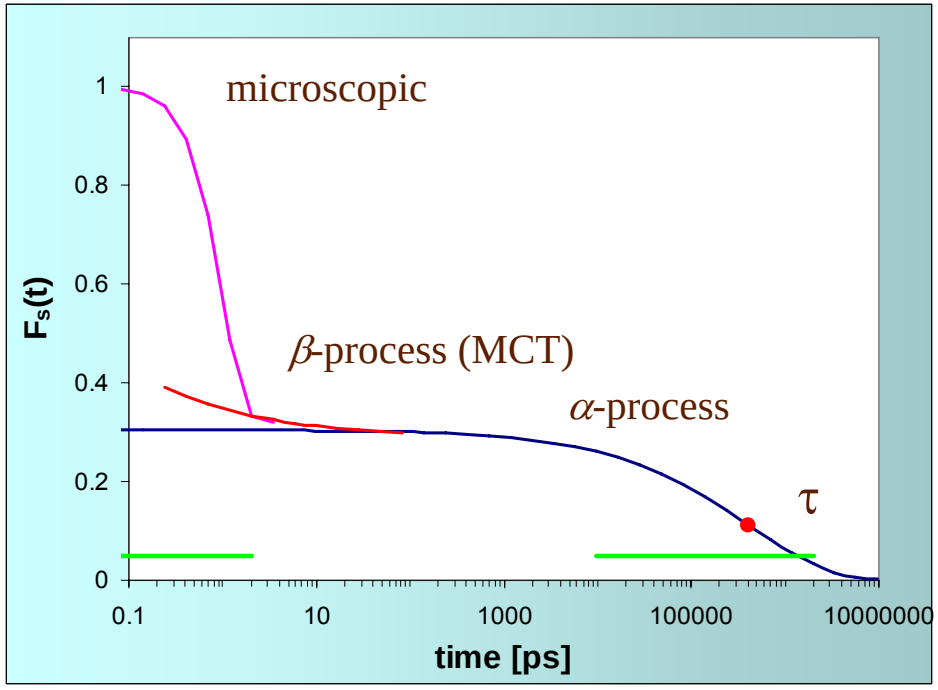

glass transition T_c: α and β process merge

Glass transition

Density correlation function on ps time-scale

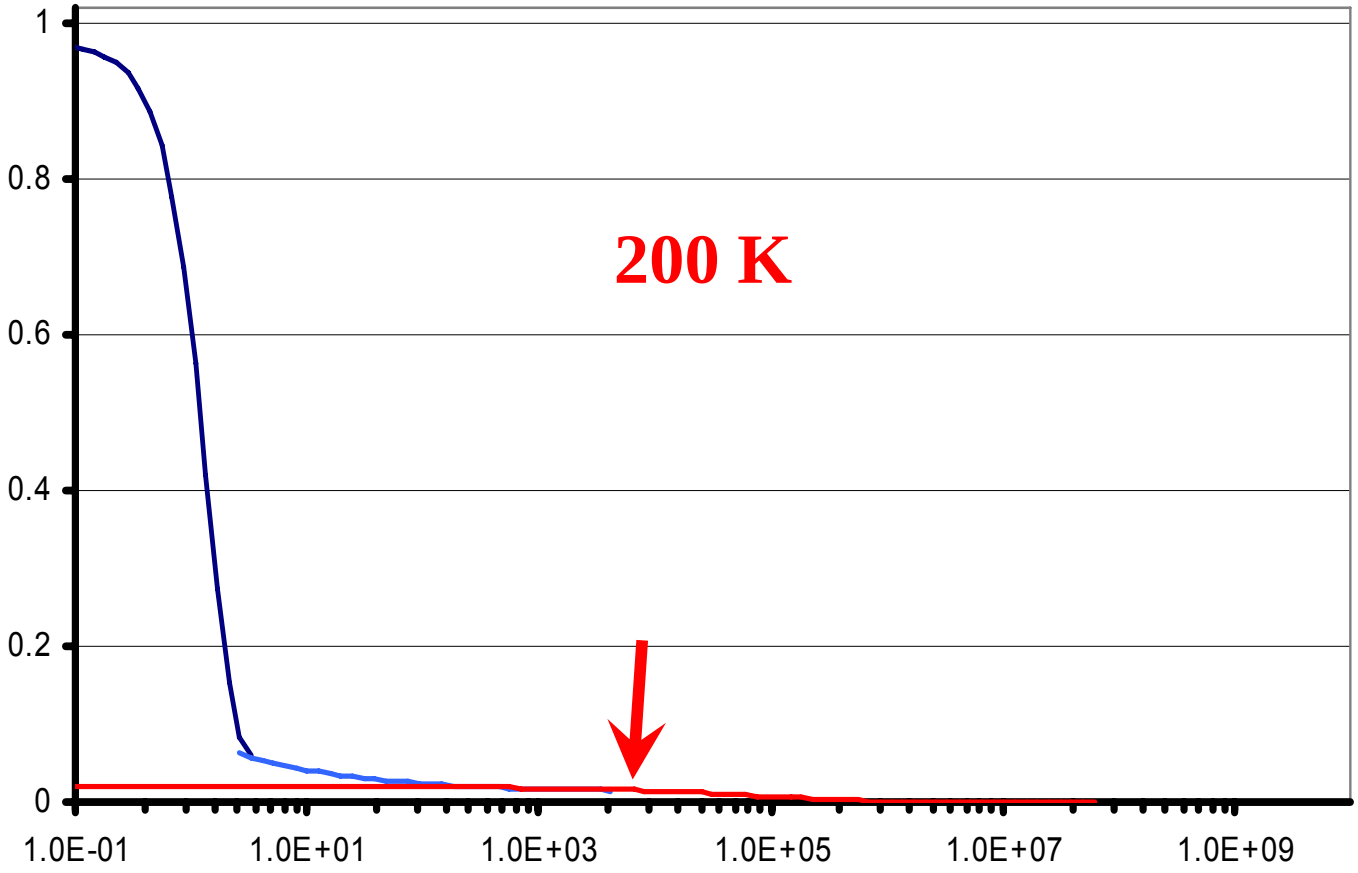

Density correlation functions and MCT

$$\phi_q(t) = \left\langle \rho_q^*(t)\rho_q(0)\right\rangle / \left\langle \left|\rho_q(0)\right|^2 \right\rangle$$

$$\ddot{\phi}_q(t) + \Omega_q^2\phi_q(t) + \Omega_q^2 \int m_q(t-t')\dot{\phi}_q(t')dt' = 0$$

Equation of motion for density correlators including „memory term“

Ergodicity - non-ergodicity transition at T_c

Power laws for correlation functions near T_c

Order parameter is the ergodicity parameter f_q

$$F_q(t) = f_q - h_q(t/\tau)^b + ... \approx f_q \exp(-t/\tau_K)^\beta$$ α-relaxation

$$F_q(t) = f_q + h_q(t_0/t)^a + ...$$ β-relaxation (cage process)

$$f_q \approx \sqrt{T_c - T}$$ Square-root singularity

Density correlation functions and MCT

$$f_q \approx \sqrt{T_c - T}$$

Square-root singularity

T_c describes a transition temperature which in contrast to T_g does not depend on experimental parameters.

The glass transition is an ergodic - non ergodic cross over

In most systems T_c is 20% higher than T_g, i.e. the transition is in the “liquid” region

The glass transition temperature T_g and T_c

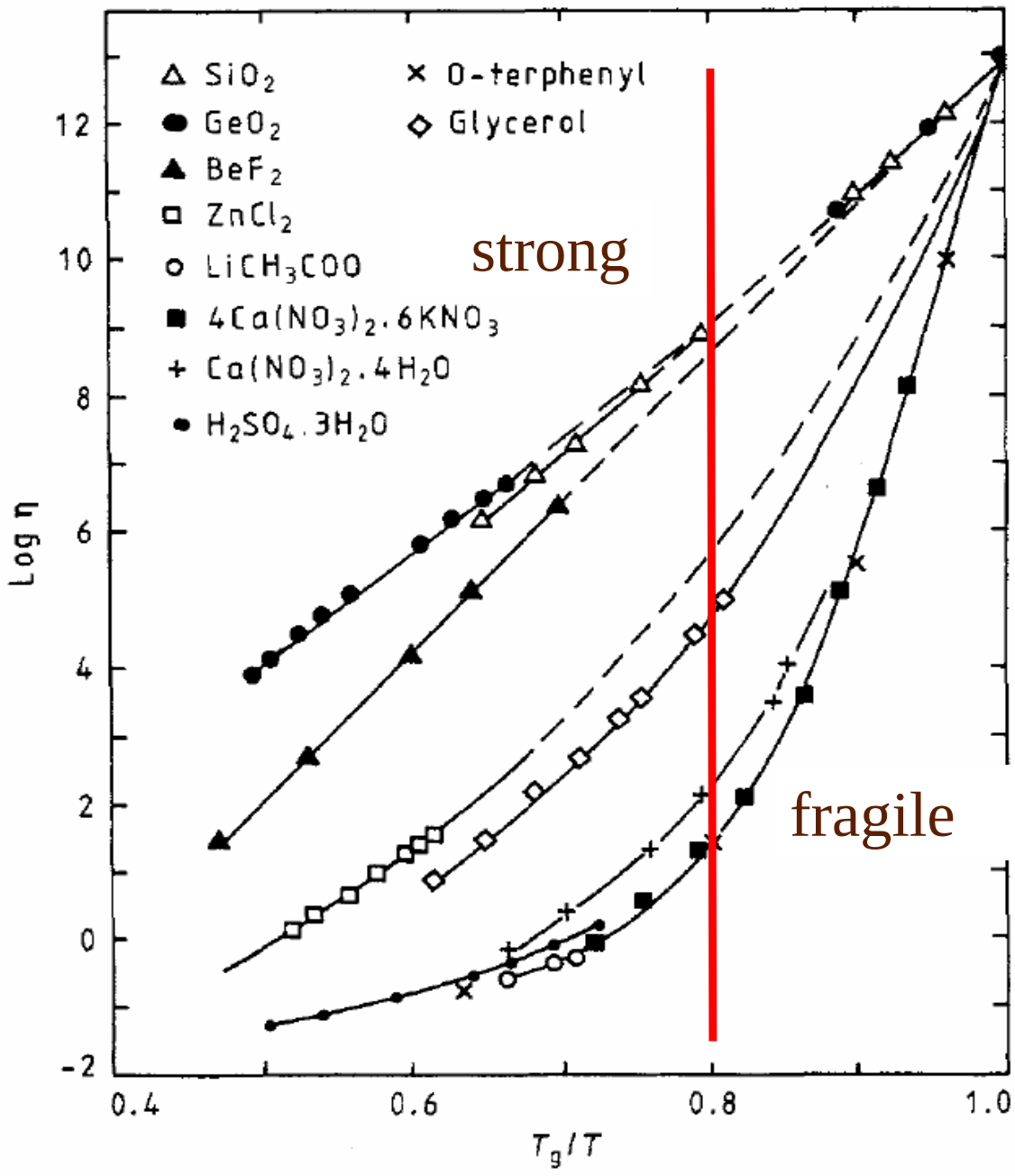

MCT results for correlation functions at the glass transition

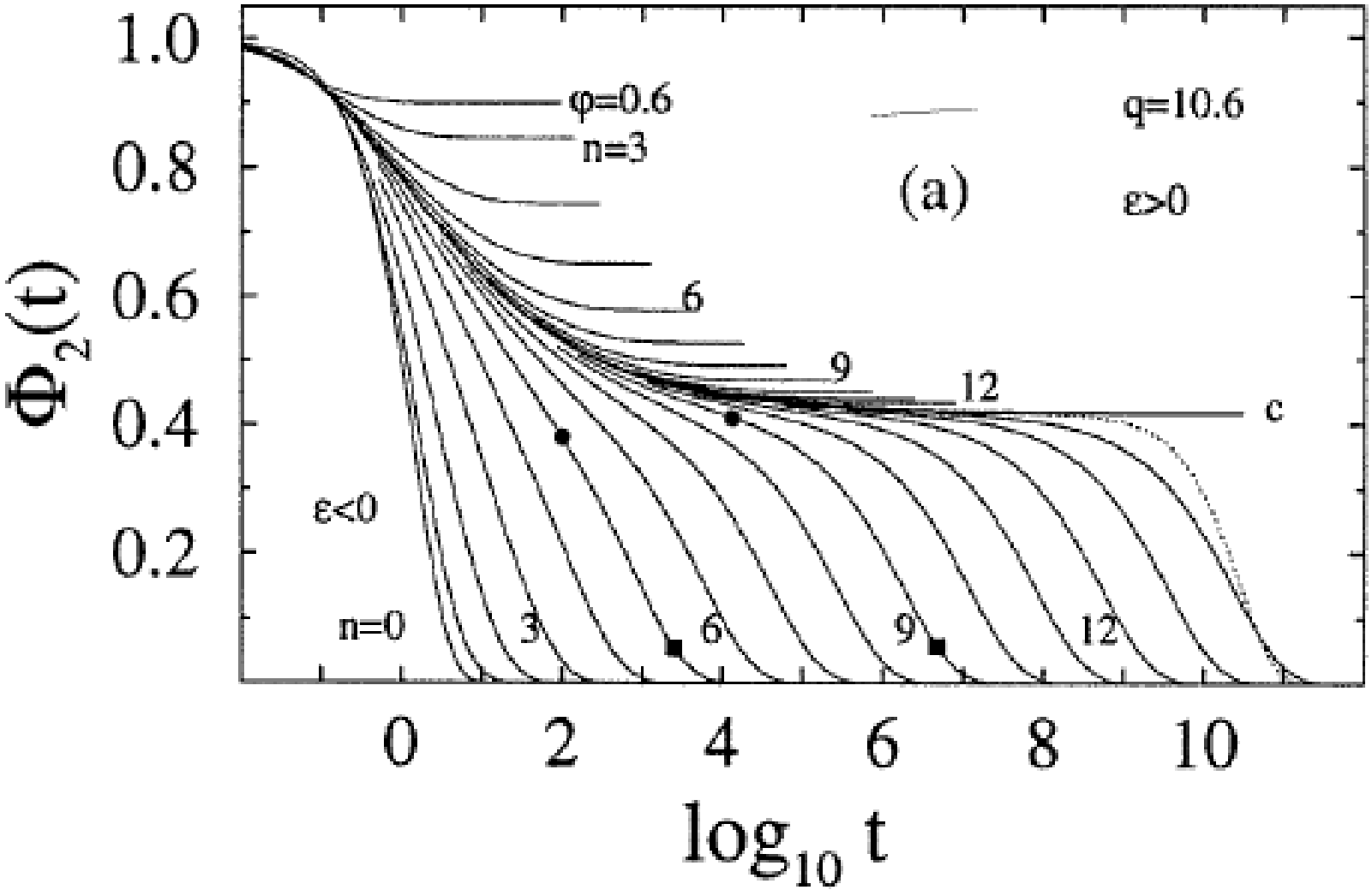

Nuclear Resonant Scattering

50 ps pulse, tuned to the transition energy
$\Delta E \approx$ meV

E = 14412.497 eV,
ΔE = 4.7 neV

^{57}Fe

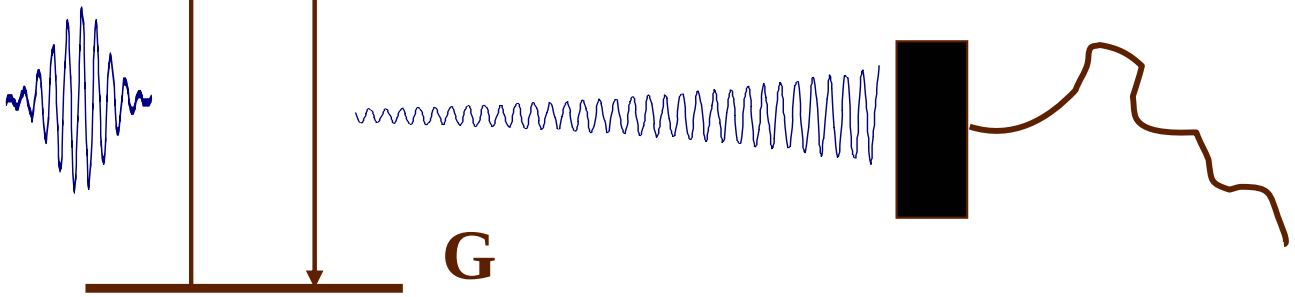

Transmitted pulse, plus resonantly scattered radiation

- $\Delta E \approx$ 10 neV
- Orders of magnitude weaker

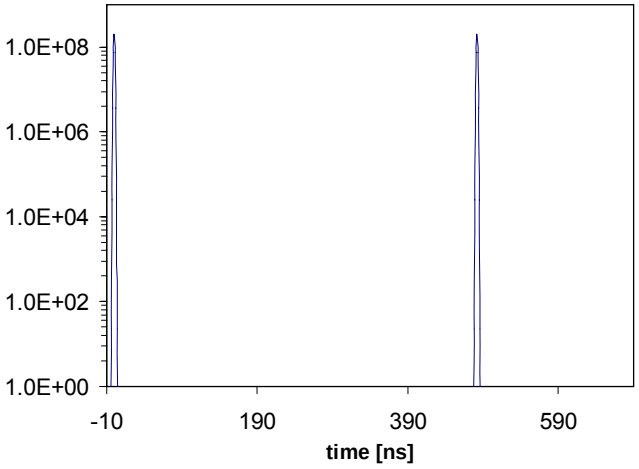

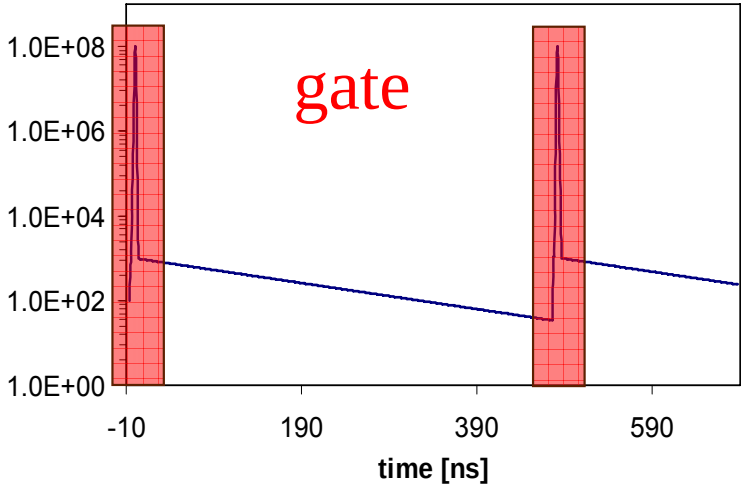

NRS set-up

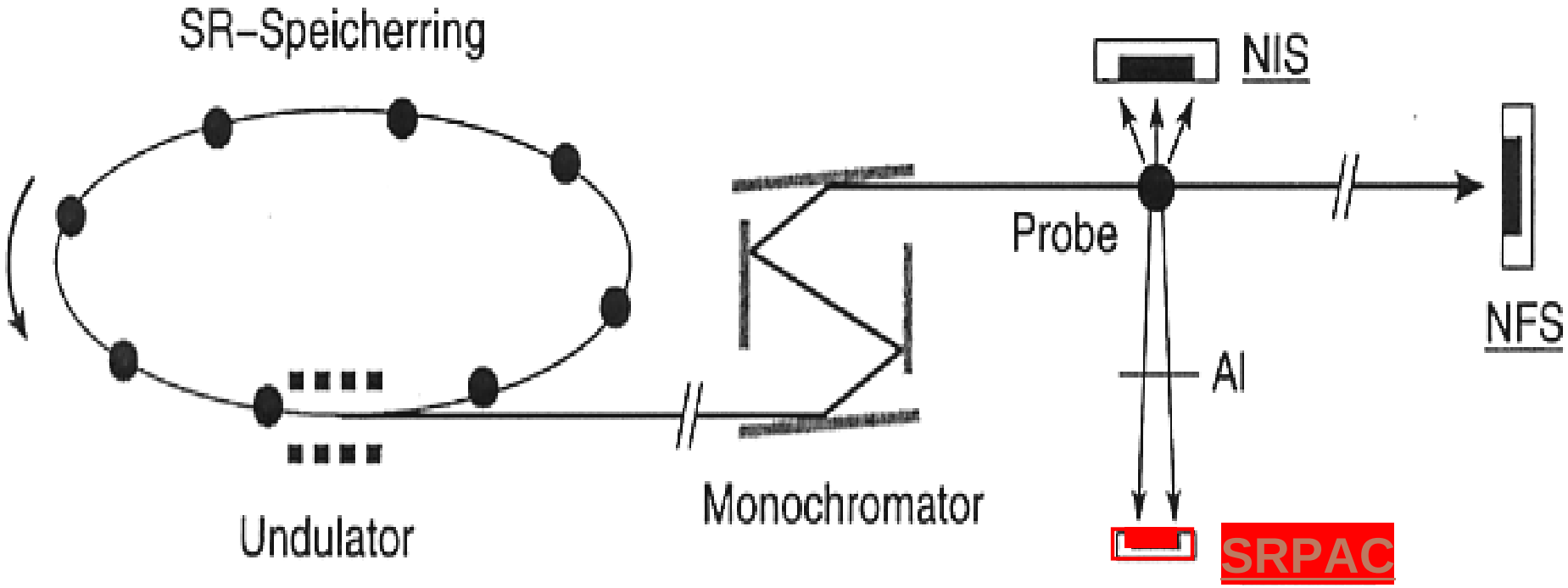
SR–Speicherring
NIS
Probe
NFS
Al
Undulator
Monochromator
SRPAC

Quasielastic nuclear resonant forward scattering

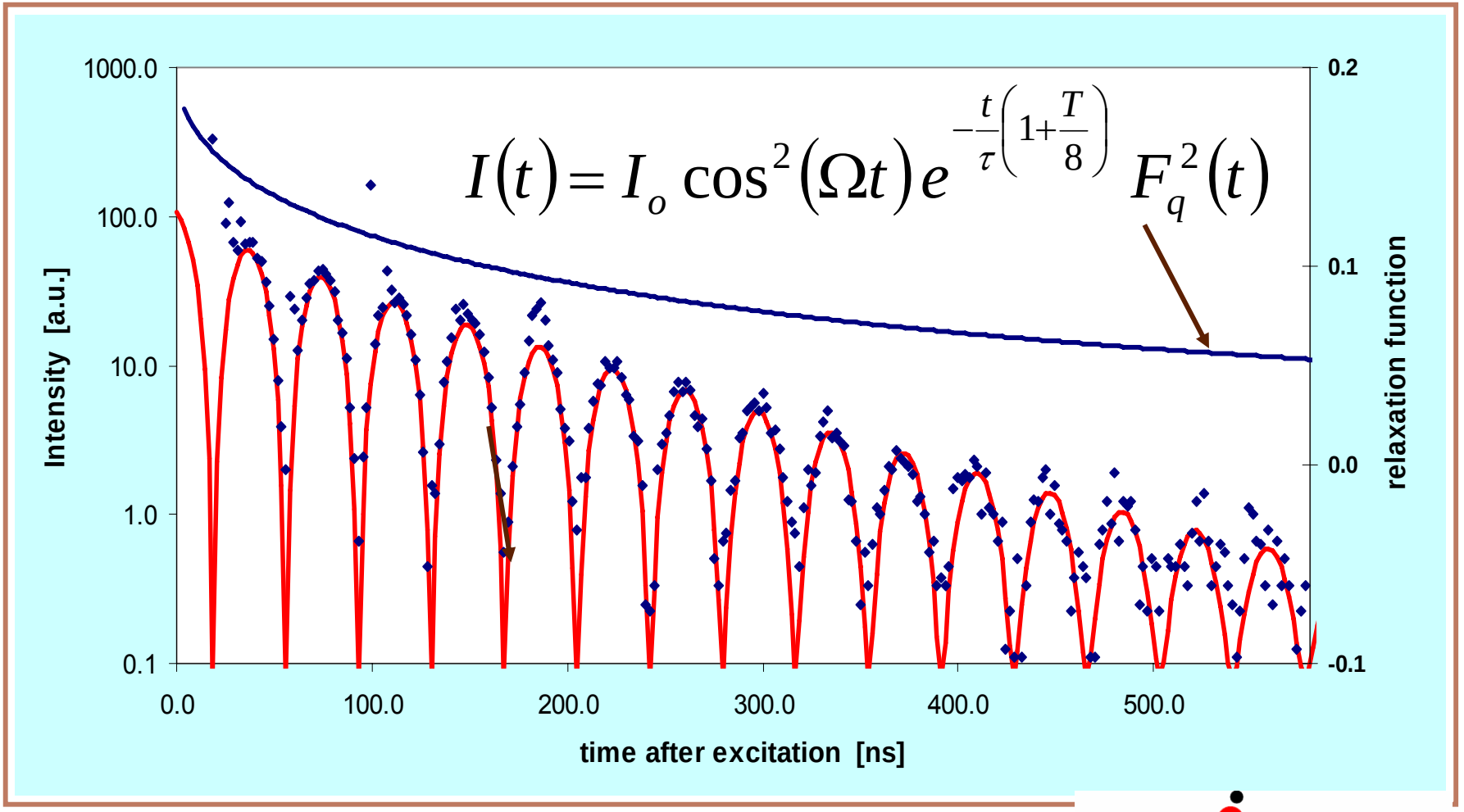

Butyl phthalate / ferrocene

Exact treatment of QNFS: I. Sergueev, HF,.. PRB 2003

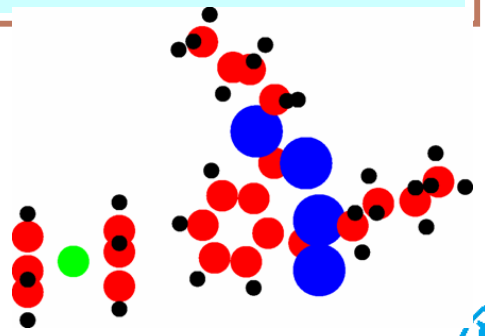

Non ergodicity parameter

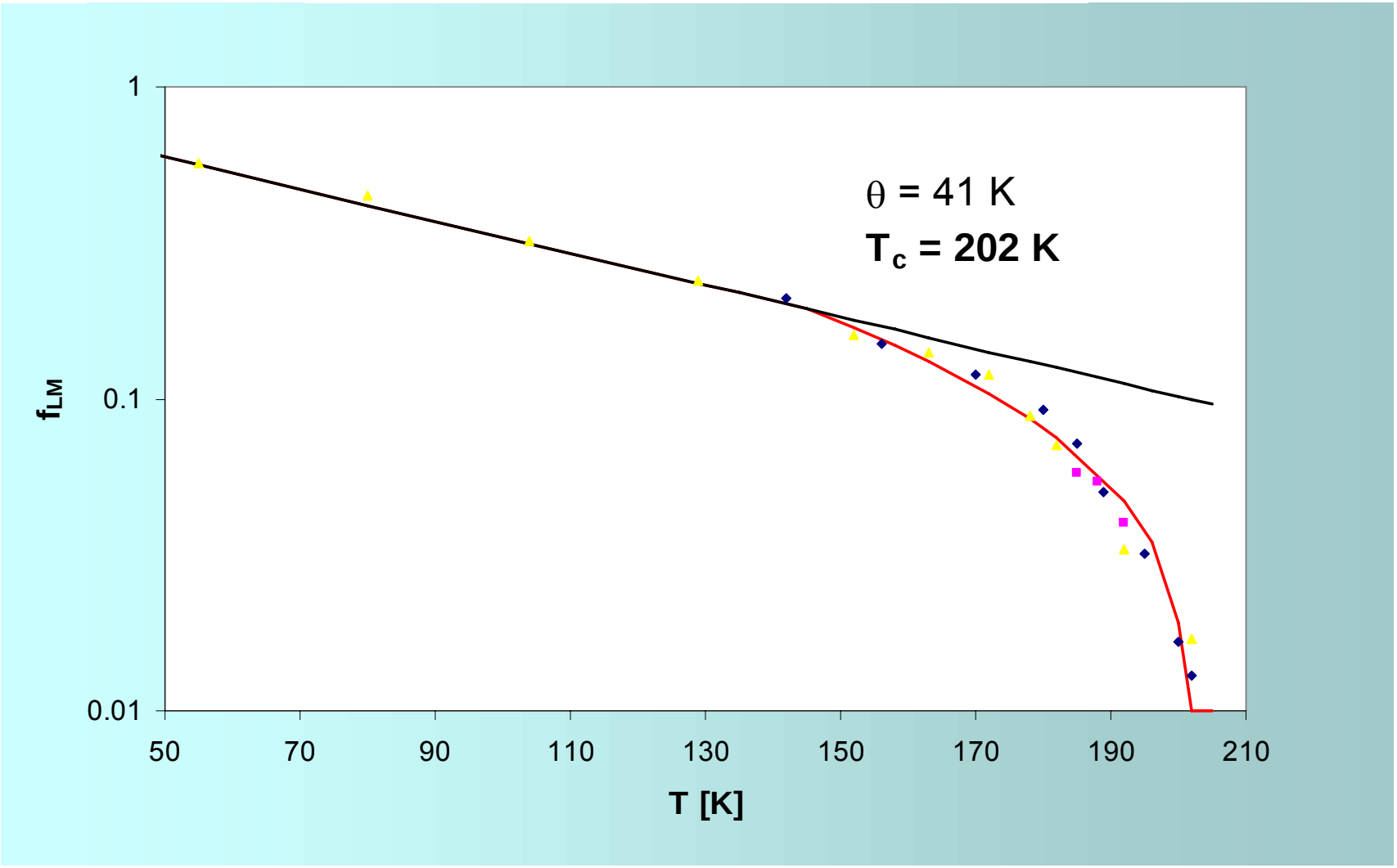

Square-root behaviour as predicted by mode-coupling theory

Stretching exponent β = 0.48, independent of T

Relaxation rates

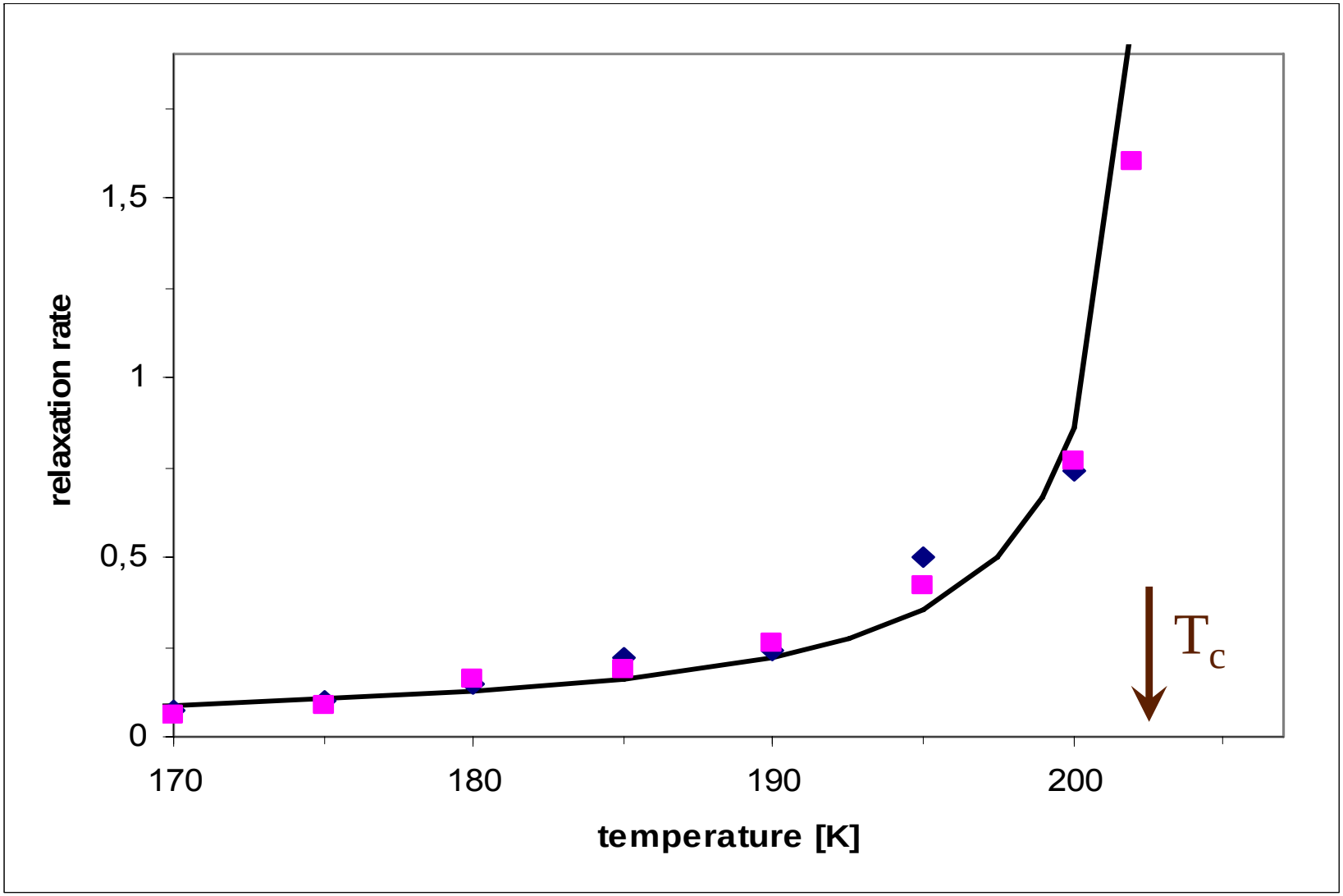

T. Asthalter, I.Sergueev, HF, et al EPJ B (2001)

Confinement

QNFS observes only the glass no signal from the matrix !

Is there a diverging length scale for the glass transition?

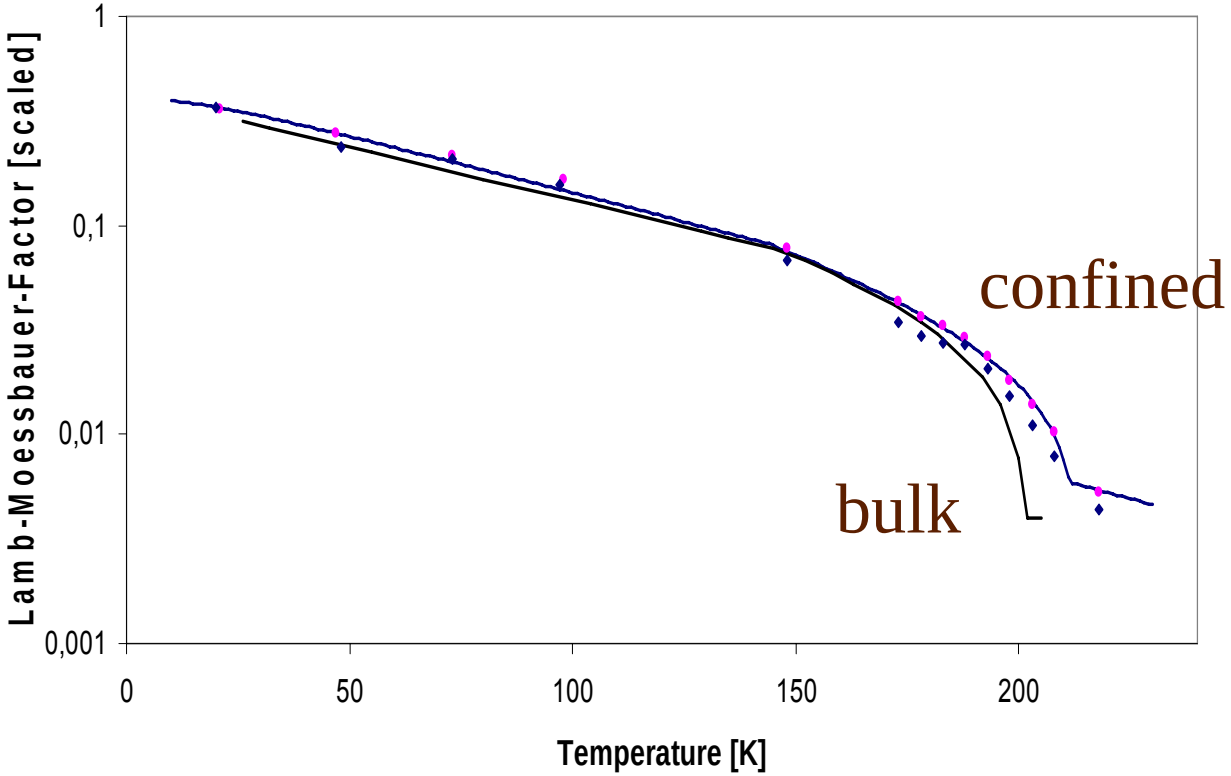

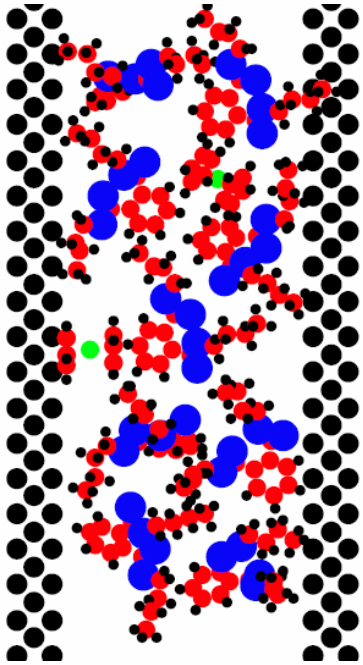

Matrix: porous silicon, structure size 5 nm.

$\Delta T_c = 11$ K

G. Wellenreuther, HF, (2003)

MD-Simulation of confined dynamics

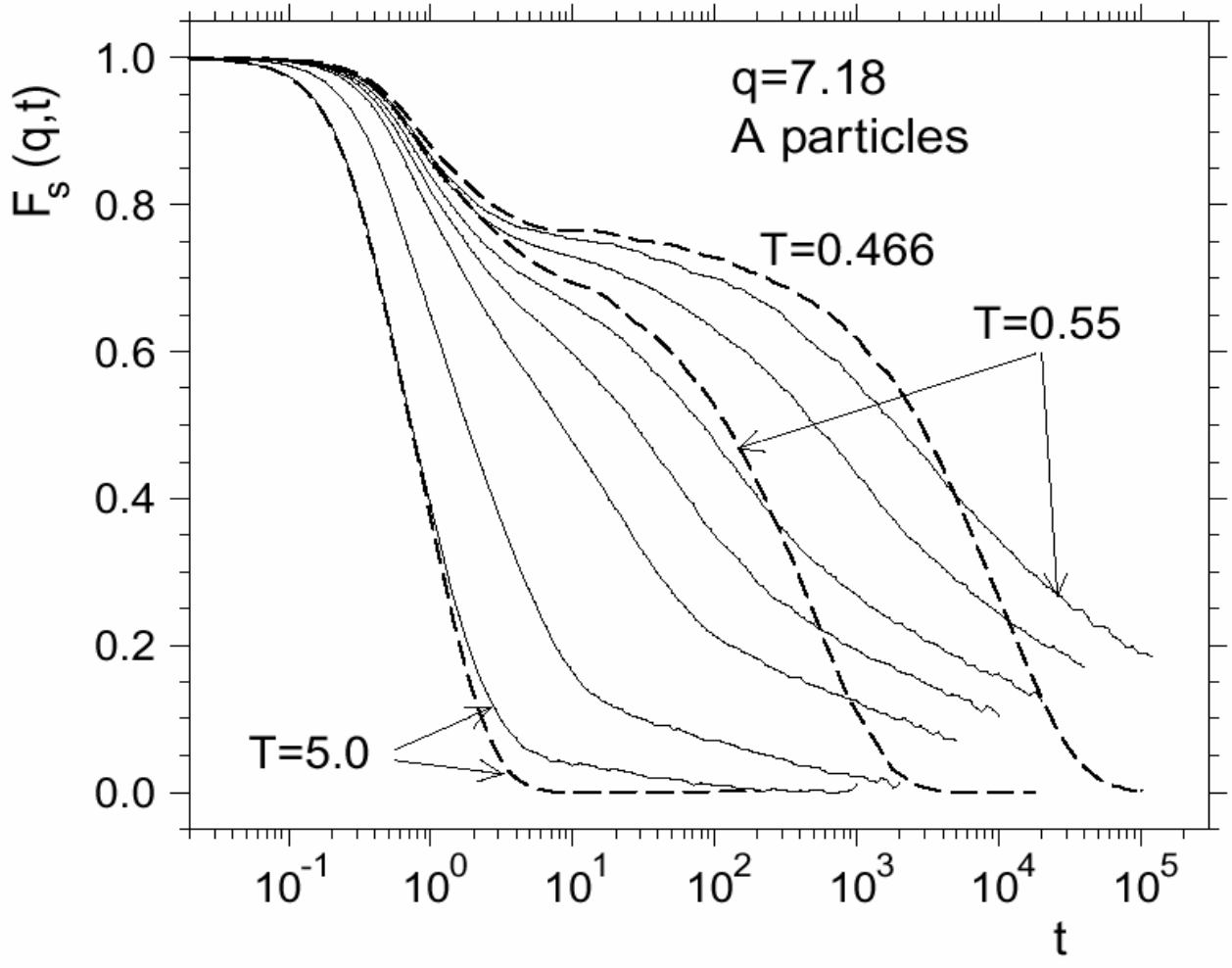

Scheidler, Kob.. EPL **52**, (2000)

Time-domain interferometry

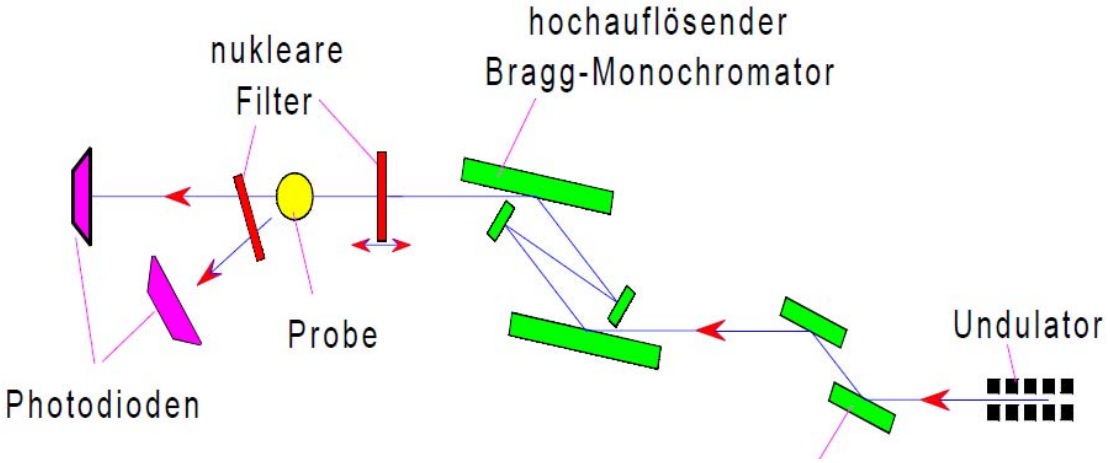

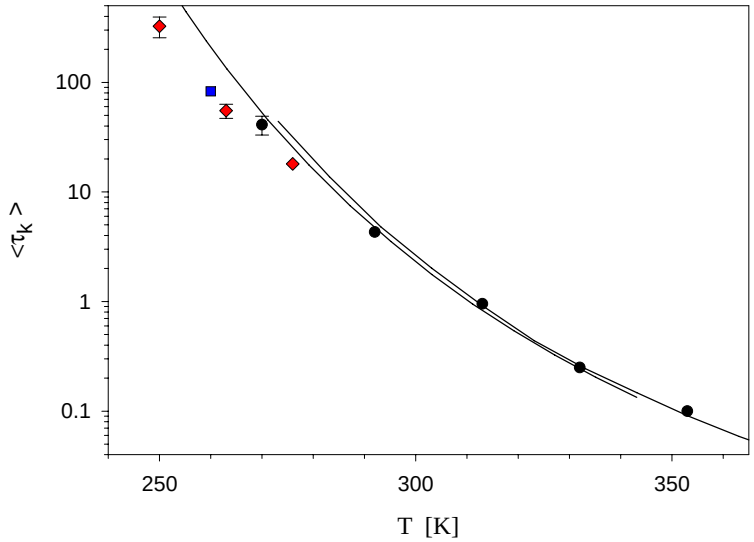

A.Q.R. Baron, HF et al. PRL (1996)

HF et al, Hyperfine Interaction (2000)

Results for glycerol

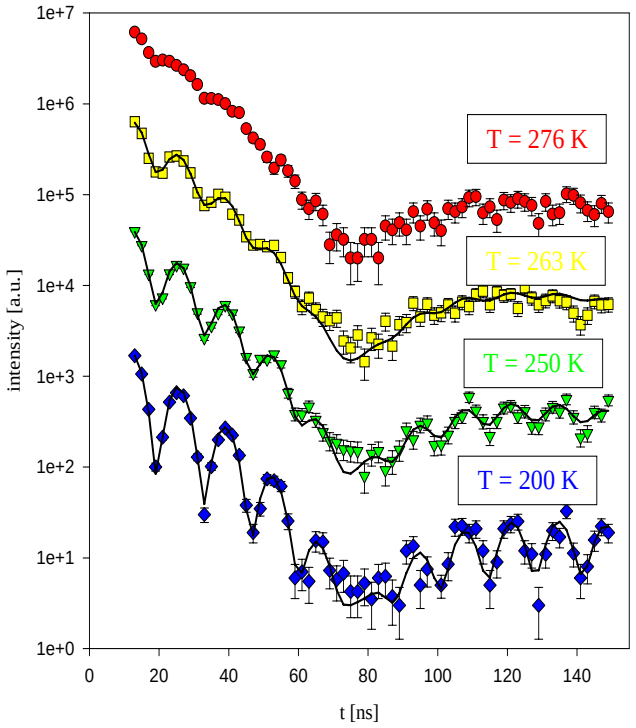

+ No resonant species

+ Free choise of q

- Low count rate

Bulk Metallic Glasses

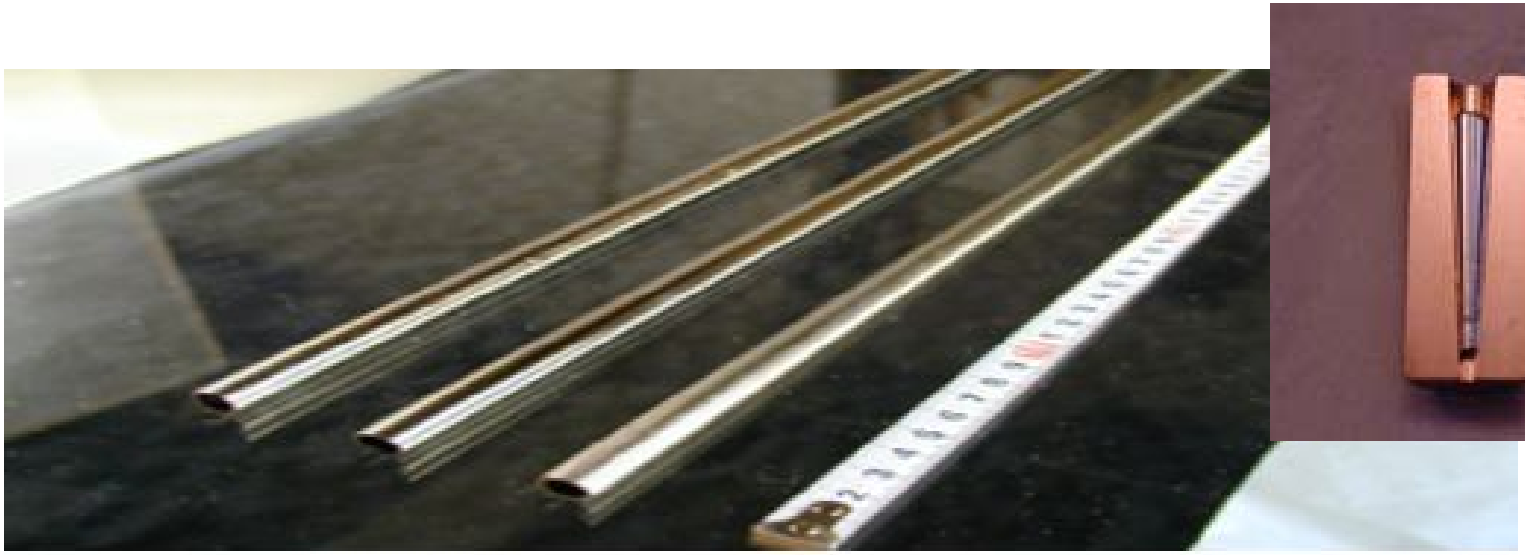

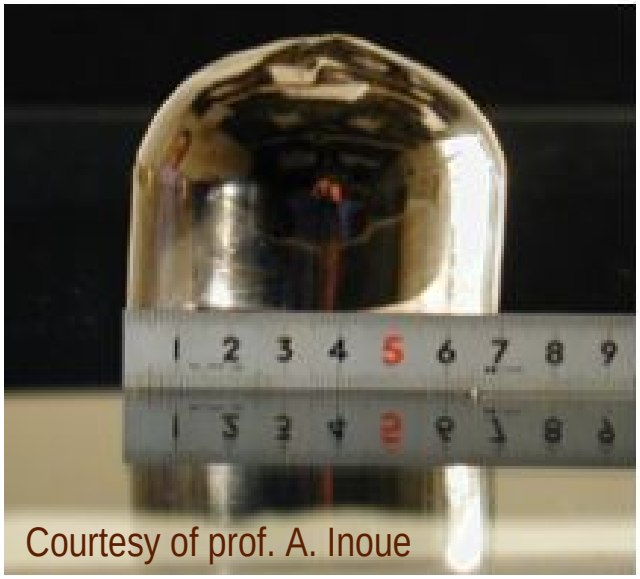

Courtesy of prof. A. Inoue

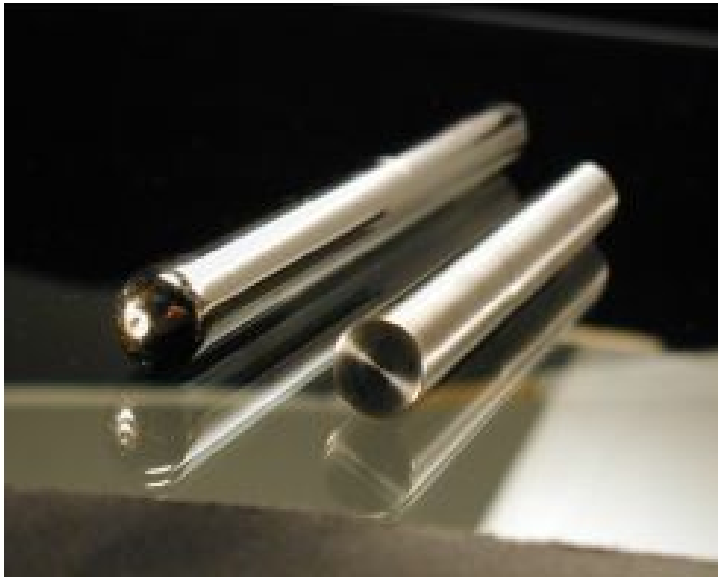

Structure vs. macroscopic properties

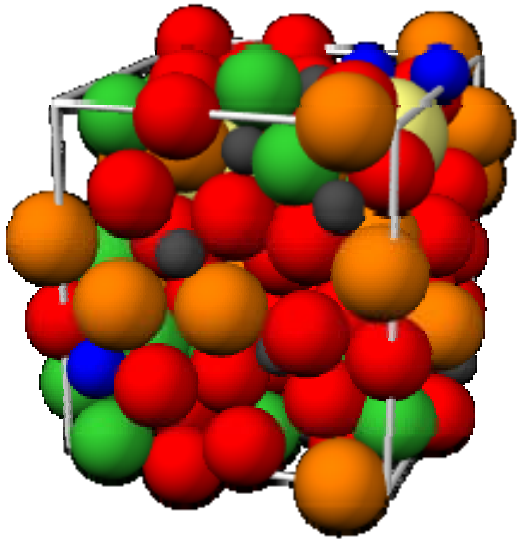

Understanding relation between the structure and macroscopic properties is important for improving performance of existing and crucial for designing novel materials

Applications

Transformers

- **low thermal losses**

Light weight compounds in space crafts

- **high specific strength**

Surface coating

- **very hard thin films**

Structure determination of amorphous materials

X-ray diffraction using high energy photons

+ high penetration depths (mm-cm)
+ relatively fast, suitable for in-situ studies
- less sensitive to elements
- ASF depend on Q

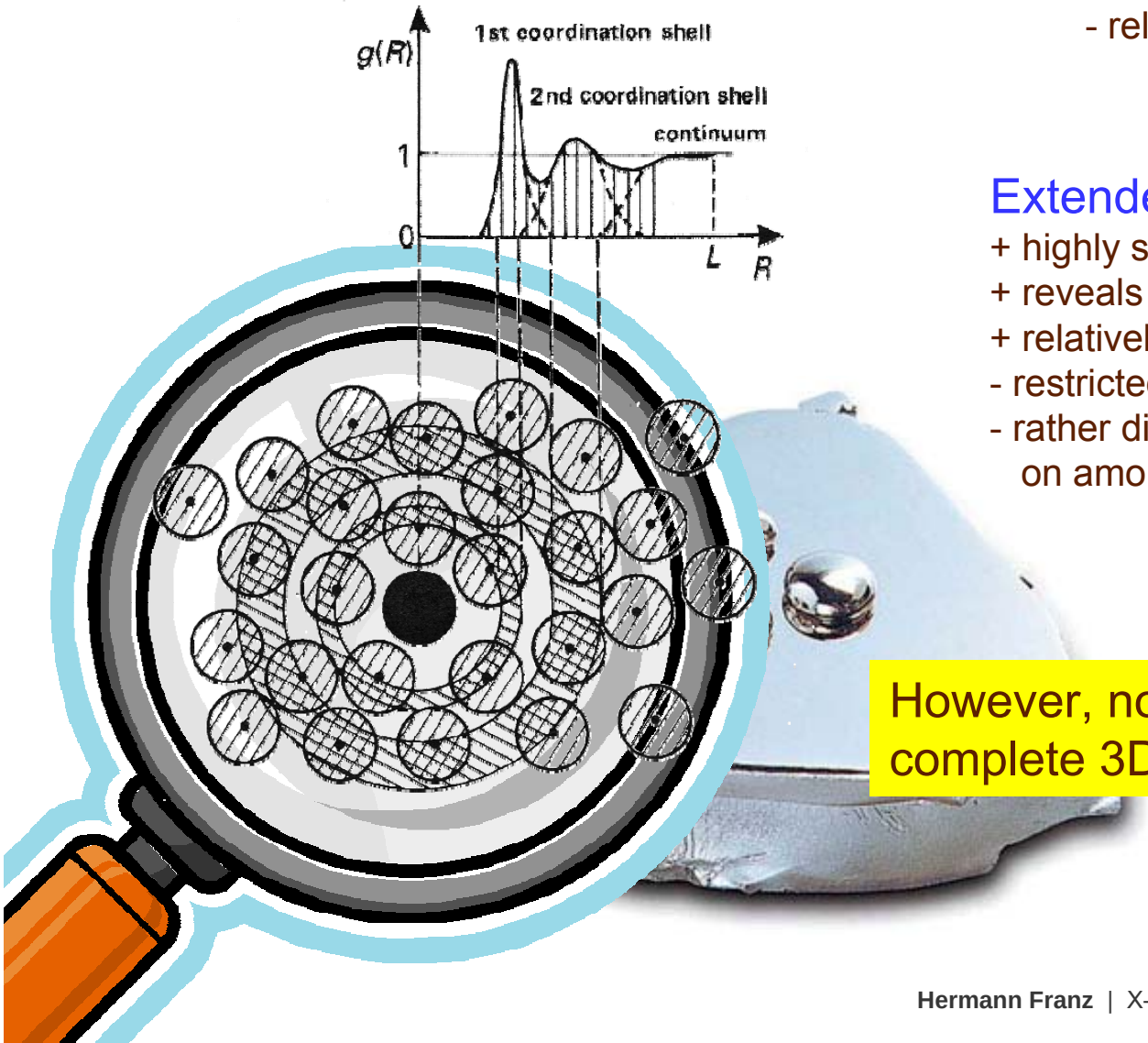

Neutron diffraction

+ sensitive to different isotopes
+ ASF do not depend on Q
+ probes magnetic state of matter
- large sample volumes
- relatively slow, not suitable for in-situ studies

Extended X-ray Absorption Spectroscopy

+ highly sensitive to elements
+ reveals local atomic configuration
+ relatively fast, suitable for in-situ studies
- restricted sample size, geometry
- rather difficult to quantitatively analyze data on amorphous samples

However, none of these techniques gives a complete 3D image of amorphous structure ☹

Reverse Monte Carlo modeling

Diffraction:

The partial $g_{ij}(r)$ functions are calculated from the ator coordinates and transformed to reciprocal space:

$$S_{ij}(Q) = \frac{4\pi\rho c_j}{Q}\int r \sin Qr(g_{ij}(r)-1)dr$$

together with a weights (for ND $f(Q)=b$)

$$w_{ij} = \frac{(2-\delta_{ij})c_i c_j f_i(Q) f_j(Q)}{\sum_{ij} c_i c_j f_i(Q) f_j(Q)}$$

are combined in total structure factor

$$S^{RMC}(Q)$$

XRD

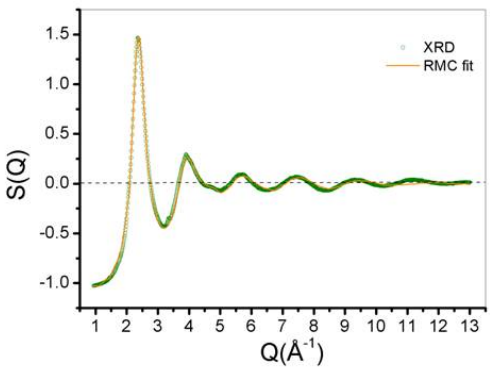

Move:

One particle is moved randomly taking into account applied constraints.

Settling:

Everything is repeated until ψ^2 begins to oscillate around a constant value.

ND

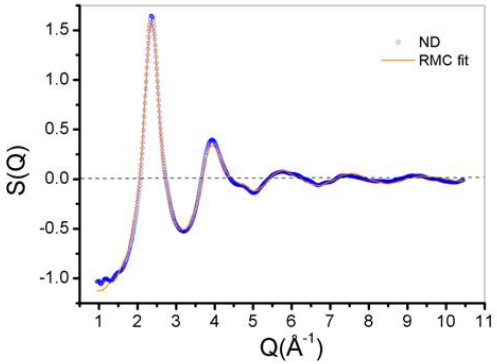

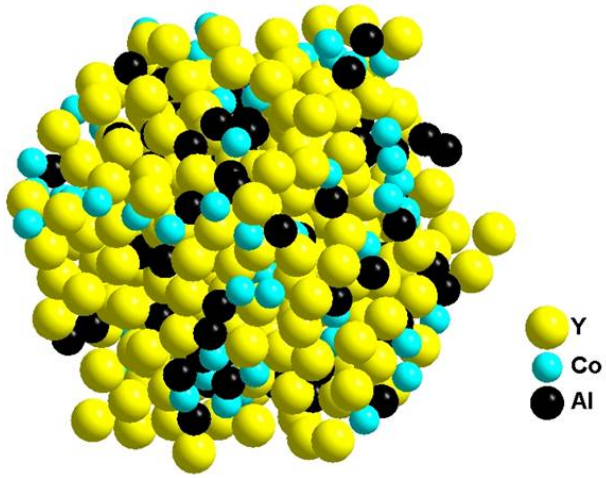

EXAFS

EXAFS:

The model of EXAFS signal $\chi_i(k)$, at the absorption edge of i-type atoms can be calculated from the g_{ij}:

$$\chi_i(k) = \sum_j 4\pi c_j \rho \int_0^\infty r^2 \gamma_{ij}(r,k) g_{ij}(r) dr$$

while γ_{ij} is the atomic pair backscattering signal

$$\gamma_{ij}(r,k) = A_{ij}(k,r)\sin(2kr + \Phi_{ij}(kr))$$

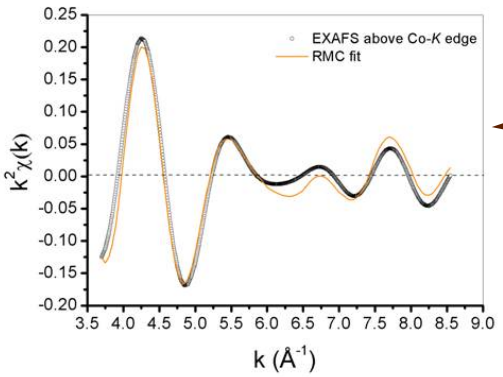

Acceptance of the move:

First the experiment-model difference is calculated

$$\psi^2 = \frac{1}{\delta}\sum_{i=1}^{m}\left[\zeta^{exp} - \zeta^{RMC}\right]^2$$

If $\psi^2_{n+1} < \psi^2_n$ the move is always accepted.
If $\psi^2_{n+1} > \psi^2_n$ the move is accepted with the probability $\exp[-(\psi^2_{n+1} - \psi^2_n)/2]$

Courtesy of Dr. K. Saksl

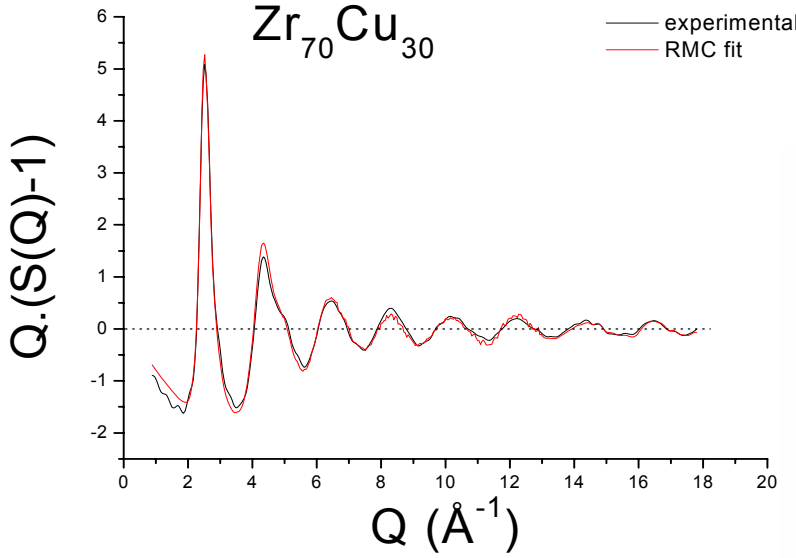
Zr70Cu30
experimental data
RMC fit
Q.(S(Q)-1)
Q (Å-1)

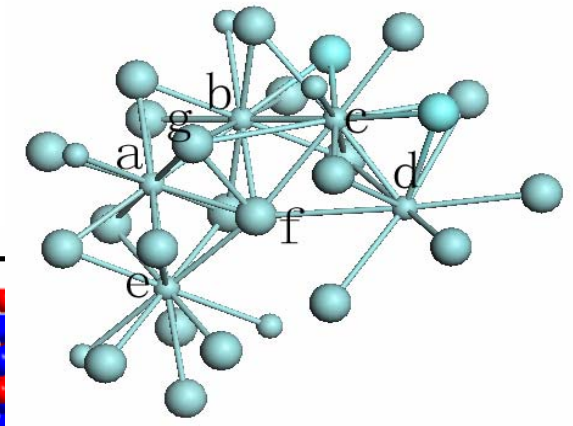
a
b
c
d
e
f
g

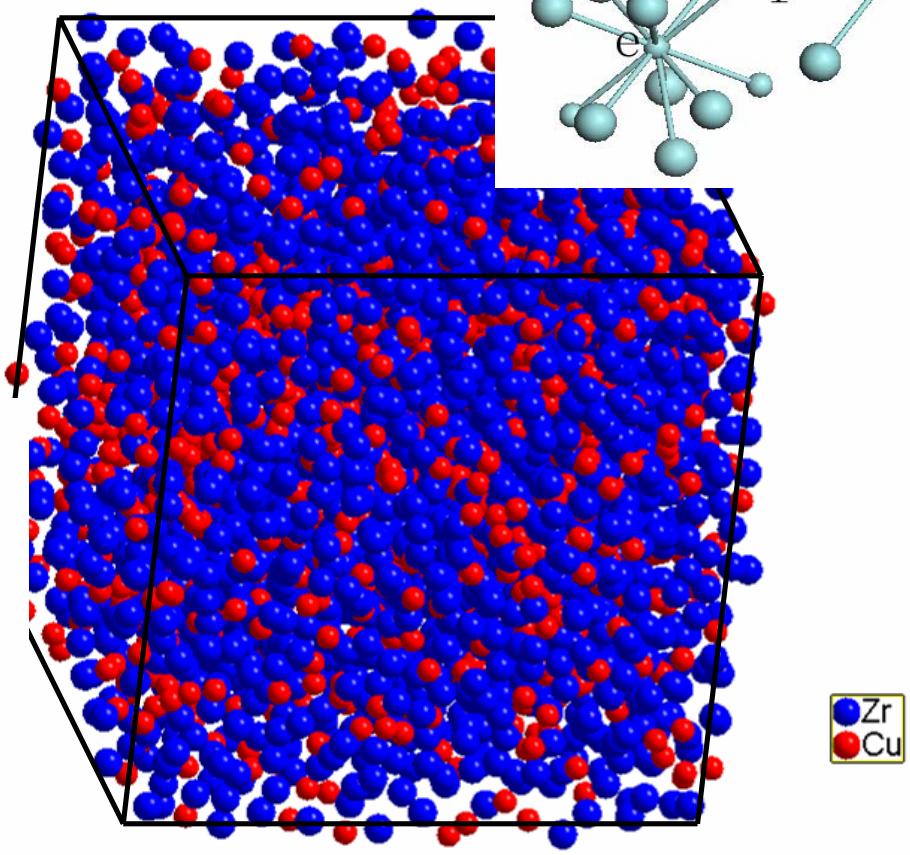
Zr
Cu

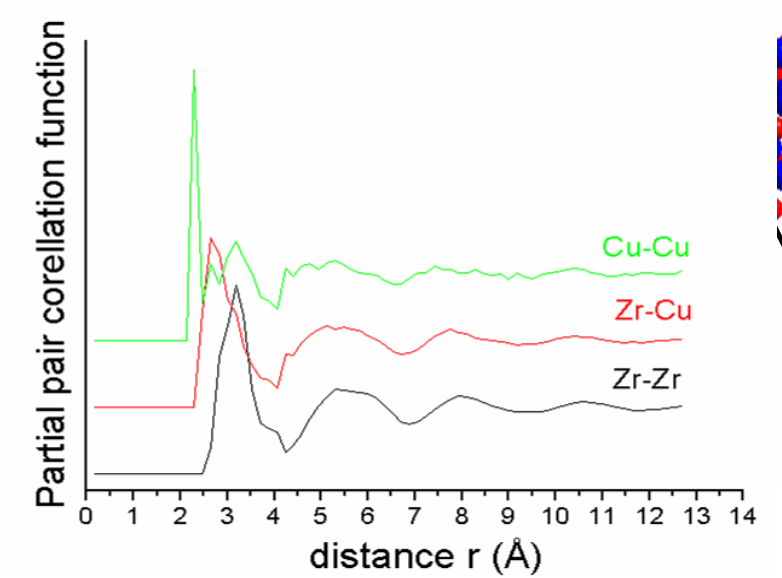
Partial pair corellation function
Cu-Cu
Zr-Cu
Zr-Zr
distance r (Å)

Systems

- Historically first alloy AuSi (1960) cooling with 10^6 K/s
- 1969 PdCuSi – only 10^3 K/s needed
- First commercial amorphous alloy, Vitreloy 1 (41.2% Zr, 13.8% Ti, 12.5% Cu, 10% Ni, 22.5% Be)
- Families of alloys
  - Pd based: PdCuNiP
  - Zr based: ZrNi, ZrTiCuNiBe (v4), ZrAlNiCuAg, ZrPd, ZrAlCu, ZrAlCuNiFe
  - La based
  - Fe based: FePCAlBGa
  - Cu based: CuZr, CuTiZr
  - Al based: AlLaNi
  - Ni based: NiZr, NiNbY

  - and many more

Systems

Table 1
The critical sizes (d_c) and thermal parameters for $Zr_{100-x-y}(Cu_zAg_{1-z})_yAl_x$ ($x = 7$–9 at.%, $y = 42$–50 at.% and $z = 0.75$–0.875) alloys, together with other BMGs reported in Refs. [20,27,28] for comparison

Alloys	Critical size	Amorphous ingots (25 g)	T_g	T_x	T_m	T_l	ΔT_x	T_{rg}	γ
$Zr_{46}Cu_{46}Al_8$	5 mm	No	715	771	978	1163	56	0.615	0.411
$Zr_{47}(Cu_{4/5}Ag_{1/5})_{46}Al_7$	<20 mm	No	704	783	1055	1242	79	0.567	0.402
$Zr_{47}(Cu_{4.5/5.5}Ag_{1/5.5})_{46}Al_7$	<20 mm	Partial	702	782	1056	1123	80	0.625	0.428
$Zr_{47}(Cu_{5/6}Ag_{1/6})_{46}Al_7$	<20 mm	Partial	703	781	1060	1125	78	0.625	0.427
$Zr_{47}(Cu_{6/7}Ag_{1/7})_{46}Al_7$	20 mm	Partial	709	774	1057	1118	65	0.634	0.424
$Zr_{45}(Cu_{4/5}Ag_{1/5})_{48}Al_7$	20 mm	Partial	710	783	1062	1208	73	0.588	0.408
$Zr_{45}(Cu_{4.5/5.5}Ag_{1/5.5})_{48}Al_7$	>20 mm	Yes	711	785	1063	1154	74	0.616	0.421
$Zr_{45}(Cu_{5/6}Ag_{1/6})_{48}Al_7$	>20 mm	Yes	713	786	1061	1159	73	0.615	0.420
$Zr_{43}(Cu_{5/6}Ag_{1/6})_{50}Al_7$	20 mm	No	738	770	1075	1127	32	0.65	0.413
$Zr_{50}(Cu_{4/5}Ag_{1/5})_{42}Al_8$	20 mm	Partial	703	774	1089	1155	71	0.609	0.417
$Zr_{50}(Cu_{5/6}Ag_{1/6})_{42}Al_8$	<20 mm	Partial	701	764	1095	1138	63	0.616	0.415
$Zr_{48}(Cu_{3/4}Ag_{1/4})_{44}Al_8$	20 mm	Partial	706	770	1092	1218	64	0.580	0.400
$Zr_{48}(Cu_{4/5}Ag_{1/5})_{44}Al_8$	>20 mm	Yes	707	762	1090	1132	55	0.625	0.414
$Zr_{48}(Cu_{4.5/5.5}Ag_{1/5.5})_{44}Al_8$	>20 mm	Yes	706	777	1089	1129	71	0.625	0.423
$Zr_{48}(Cu_{5/6}Ag_{1/6})_{44}Al_8$	>20 mm	Yes	705	778	1090	1122	73	0.628	0.426
$Zr_{48}(Cu_{6/7}Ag_{1/7})_{44}Al_8$	>20 mm	Yes	706	778	1089	1127	72	0.626	0.424
$Zr_{48}(Cu_{7/8}Ag_{1/8})_{44}Al_8$	20 mm	Partial	707	779	1095	1127	72	0.627	0.425
$Zr_{46}(Cu_{4/5}Ag_{1/5})_{46}Al_8$	>20 mm	Yes	710	776	1091	1228	66	0.578	0.400
$Zr_{46}(Cu_{4.5/5.5}Ag_{1/5.5})_{46}Al_8$	>20 mm	Yes	703	775	1088	1126	72	0.624	0.424
$Zr_{46}(Cu_{4.5/5.5}Ag_{1/5.5})_{46}Al_8$ ingots	>20 mm	Yes	704	776	1089	1130	72	0.623	0.423
$Zr_{46}(Cu_{5/6}Ag_{1/6})_{46}Al_8$	>20 mm	Partial	710	778	1088	1120	68	0.634	0.425
$Zr_{53}(Cu_{5/6}Ag_{1/6})_{38}Al_9$	20 mm	Partial	711	767	1089	1129	56	0.63	0.417
$Zr_{51}(Cu_{4.5/5.5}Ag_{1/5.5})_{40}Al_9$	20 mm	Partial	703	758	1092	1144	55	0.615	0.410
$Zr_{49}(Cu_{5/6}Ag_{1/6})_{42}Al_9$	20 mm	Partial	708	767	1092	1242	59	0.57	0.393
$Cu_{43}Zr_{43}Al_7Ag_7$ [27]	8 mm	–	722	794	1125	–	72	–	–
$Zr_{41.2}Ti_{13.8}Cu_{12.5}Ni_{10}Be_{22.5}$ [28]	25 mm	–	623	672	932	996	49	0.67	0.415
$Pd_{40}Cu_{30}Ni_{10}P_{20}$ [28]	72 mm	–	575	670	804	840	95	0.72	0.473
$La_{62}Al_{14}Cu_{11.3}Ag_{2.7}Ni_5Co_5$ [20]	>20 mm	–	422	482	642	727	60	0.580	0.419
$La_{65}Al_{14}Cu_{9.2}Ag_{1.8}Ni_5Co_5$ [20]	35 mm	–	419	459	641	687	40	0.610	0.415

"Yes", "partial" and "no" are roughly defined by eyes for ingots having volume fractions of larger than about 80%, 30–80% and less than about 30% for the amorphous component, respectively.

Favorable conditions for glass formation

Couple of empirical rules in literature

However up to now still empirical (trail and error) development

- **Three or more alloy components**
- **Very different atomic radii**
- **Negative heat of mixing**
- **Low eutectic**
- **Competing crystalline phases**

> **There is no microscopic theory describing the formation of BMG**

Magnetic properties

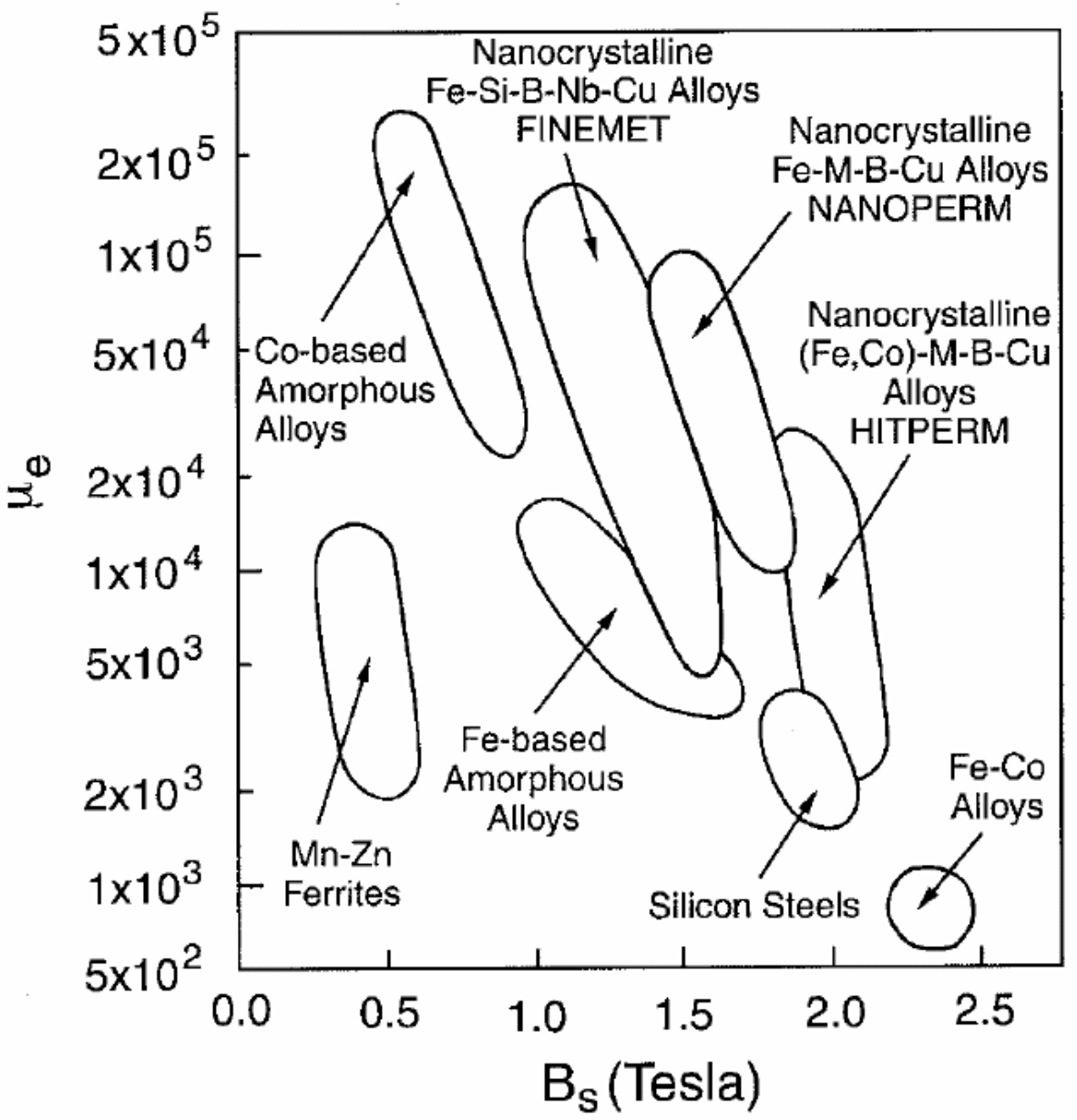

High strength

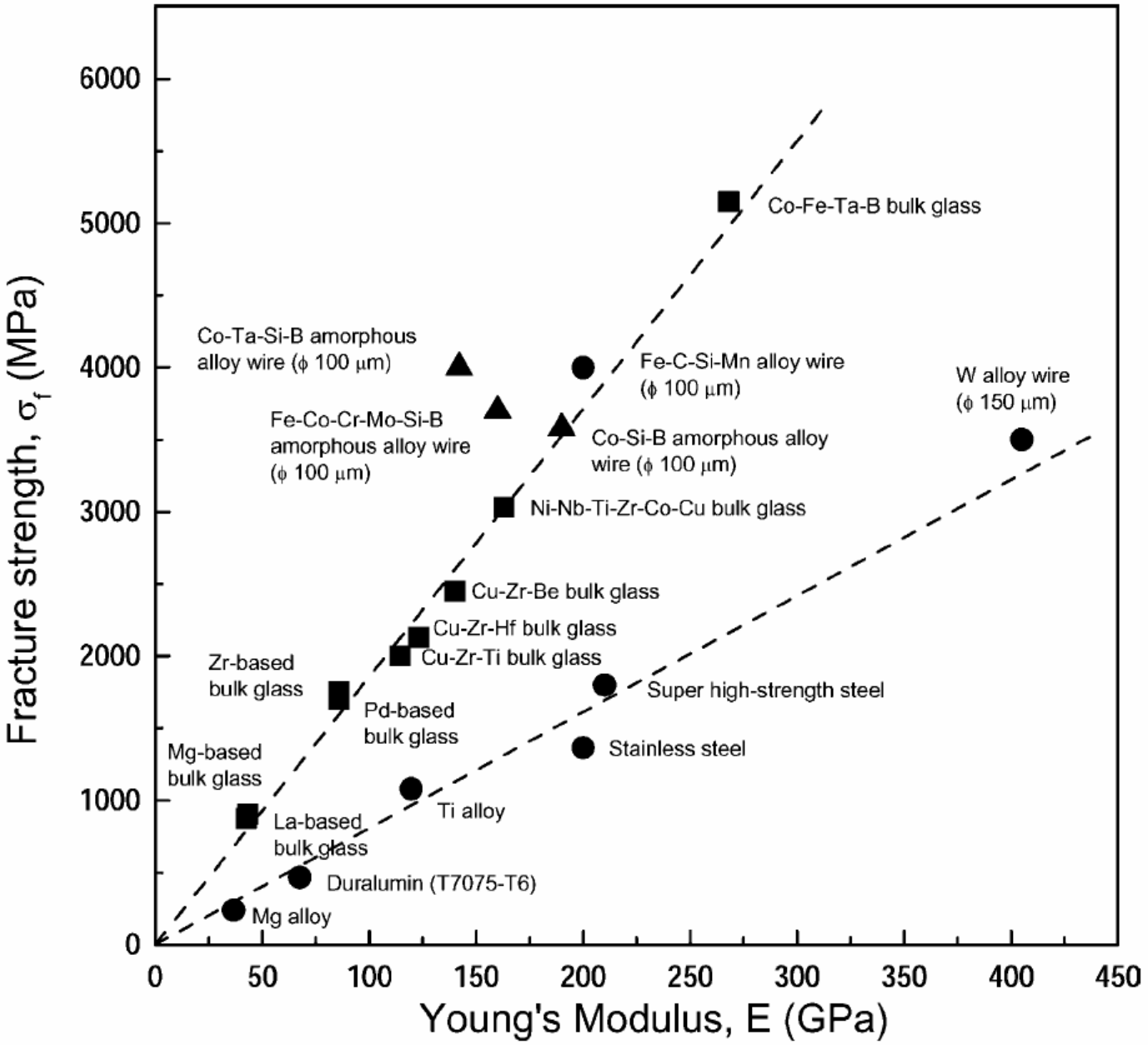

Sample preparation - melt spinning

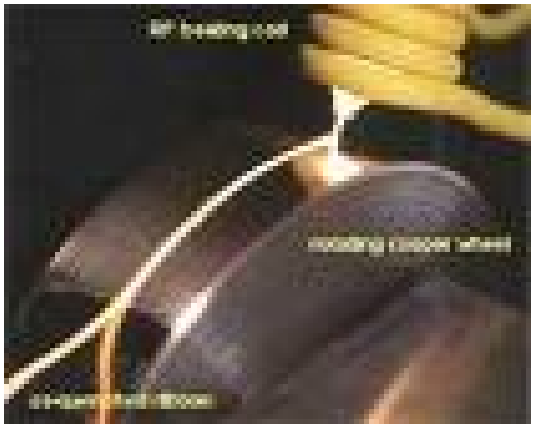

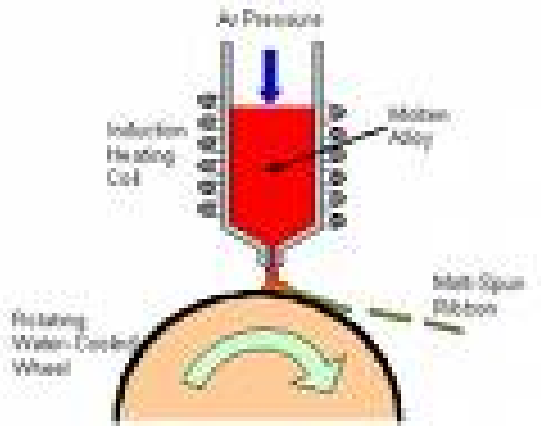

Rather wide spread

Cooling rate up to 10^5 K/s

Production of large quantities

However only thin films (couple of 10 μm)

Sample preparation - splat cooling

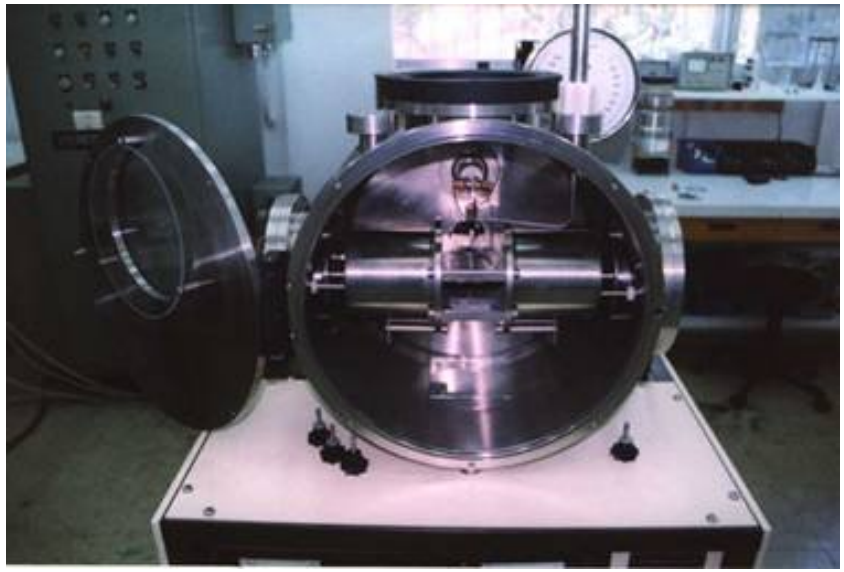

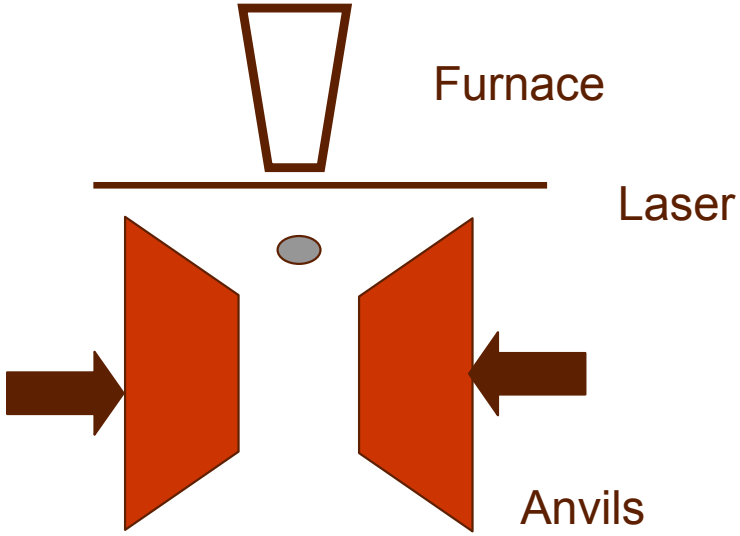

Rather wide spread

Cooling rate up to 10^6 K/s

Production of small quantities

Only thin disks (couple of 10 μm)

In-situ tensile experiments

Tensile/compression module

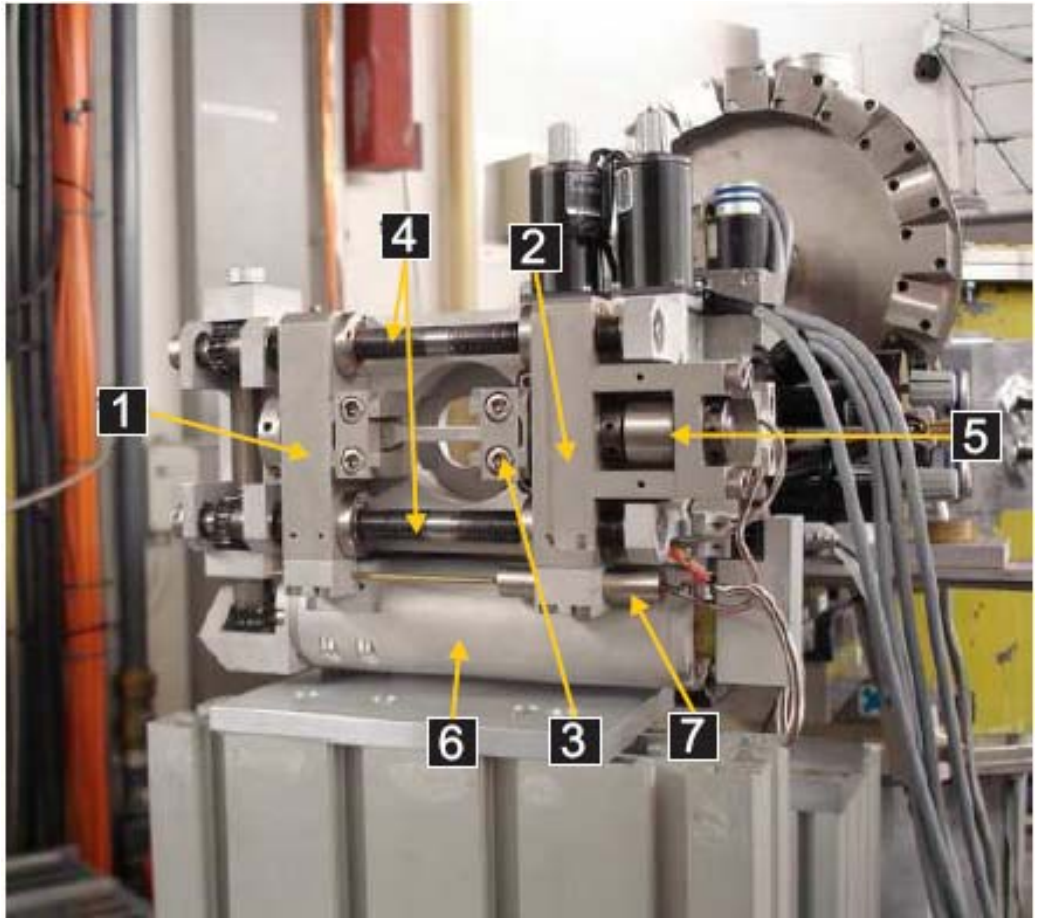

[1] - rear yoke, [2] - front yoke, [3] - clamping,
[4] - leading screws, [5] -load cell, [6] - motor,
[7] - displacement gauge

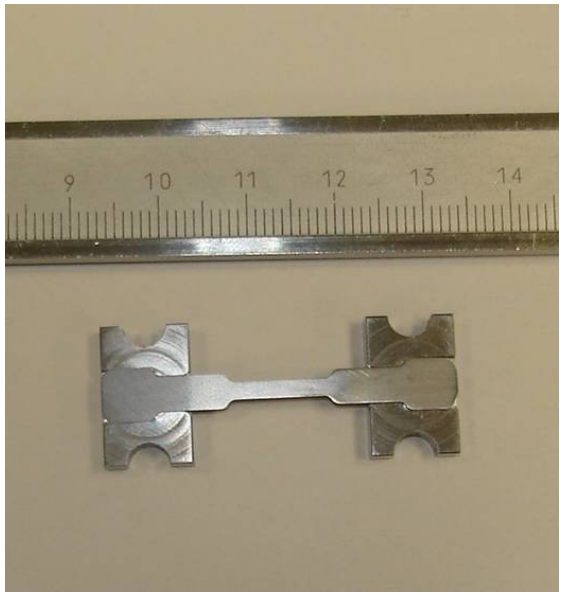

$Zr_{64.13}Cu_{15.75}Ni_{10.12}Al_{10}$

Y. H. Liu, G. Wang, R. J. Wang, D. Q. Zhao, M. X. Pan, and W. H. Wang, Science **315**, 1385 2007.

In-situ tensile experiments using high-energy XRD

BW5 is dedicated to X-ray scattering experiments using high-energy photons (**60 - 150 keV**).

The **large penetration depth** at these energies of typically **sereral mm to cm** allows the investigation of bulk materials and complex sample environments.

The experimental station is equipped with a triple axis diffractometer and an **image plate** camera.

Parameters:

- wavelength λ = 0.12398 Å (100 keV)
- crossection of collimated beam 1mm^2
- exposure time 10 s
- XRD in transmission mode
- 2D ma345 image plate detector used in symetric mode

In-situ tensile experiments

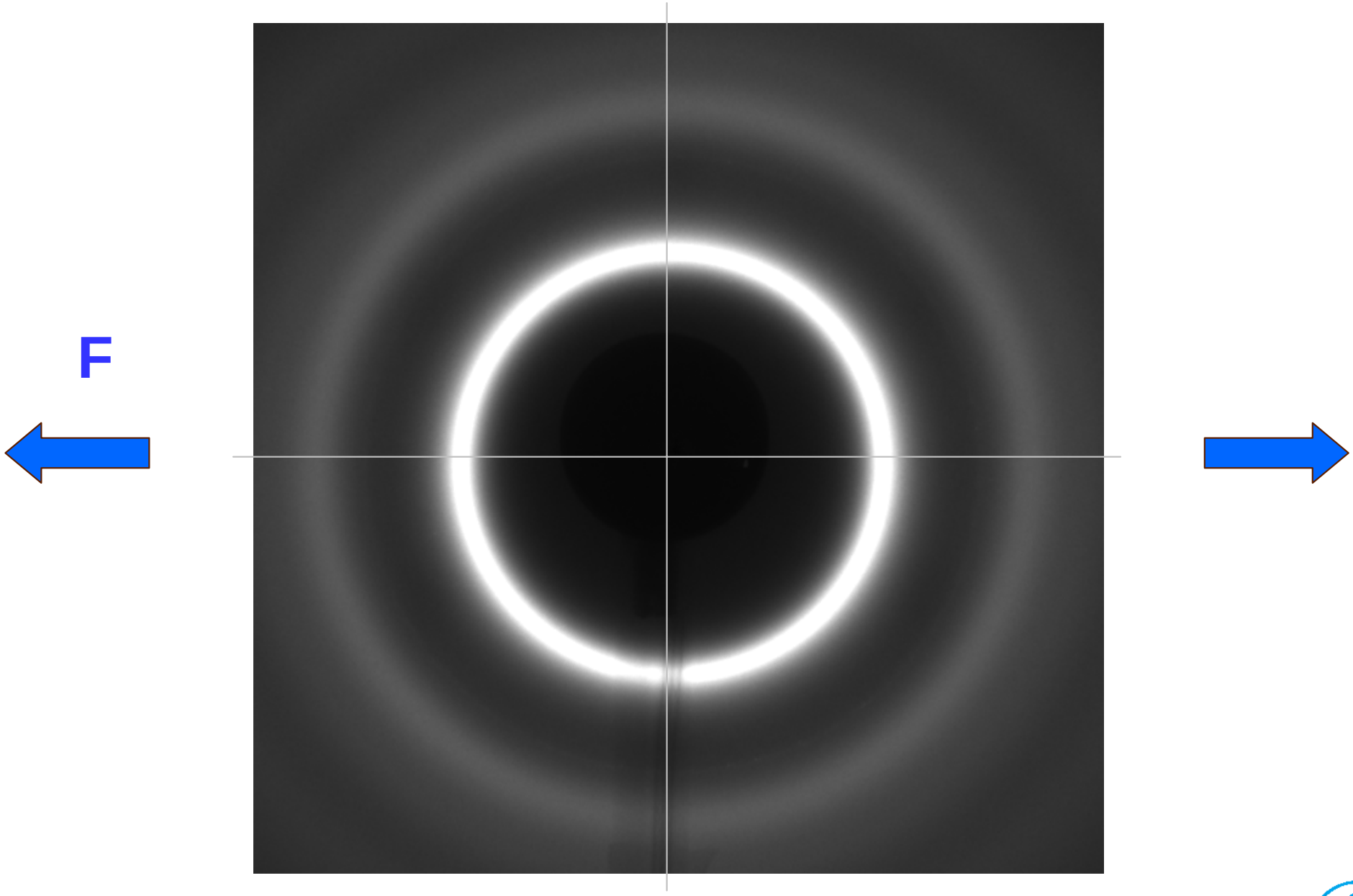

Courtesy J. Bednarcik

Determination of deformation state by XRD

The symmetric circular diffraction pattern is characterized with respect to the polar coordinates (*s*, η). By dividing the η-range of 0 to 2π into 36 segments, one obtains symmetrized intensity distributions

$$I'_i(Q,\eta_i) = \int_{\eta_i-\pi/36}^{\eta_i+\pi/36} [I(Q,\eta) + I(Q,\eta+\pi)]\, d\eta$$

with i = 1…18, where the wave-vector transfer $Q = Q(s)$ is defined by

$$Q(s) = \frac{4\pi}{\lambda} \sin\left(\frac{1}{2} arctg\left(\frac{s}{D}\right)\right)$$

in which λ denotes the wavelength, D refers to the sample-to-detector distance and s represents the distance from the origin of the polar coordinate system.

The relative change of the position of the principal peak upon applying an external stress defines the strain

$$\varepsilon_i(\eta_i,\sigma) = \frac{q(\eta_i,0) - q(\eta_i,\sigma)}{q(\eta_i,\sigma)}$$

H. F. Poulsen et al., *Nat. Mater.* **4** 33-35 (2005)

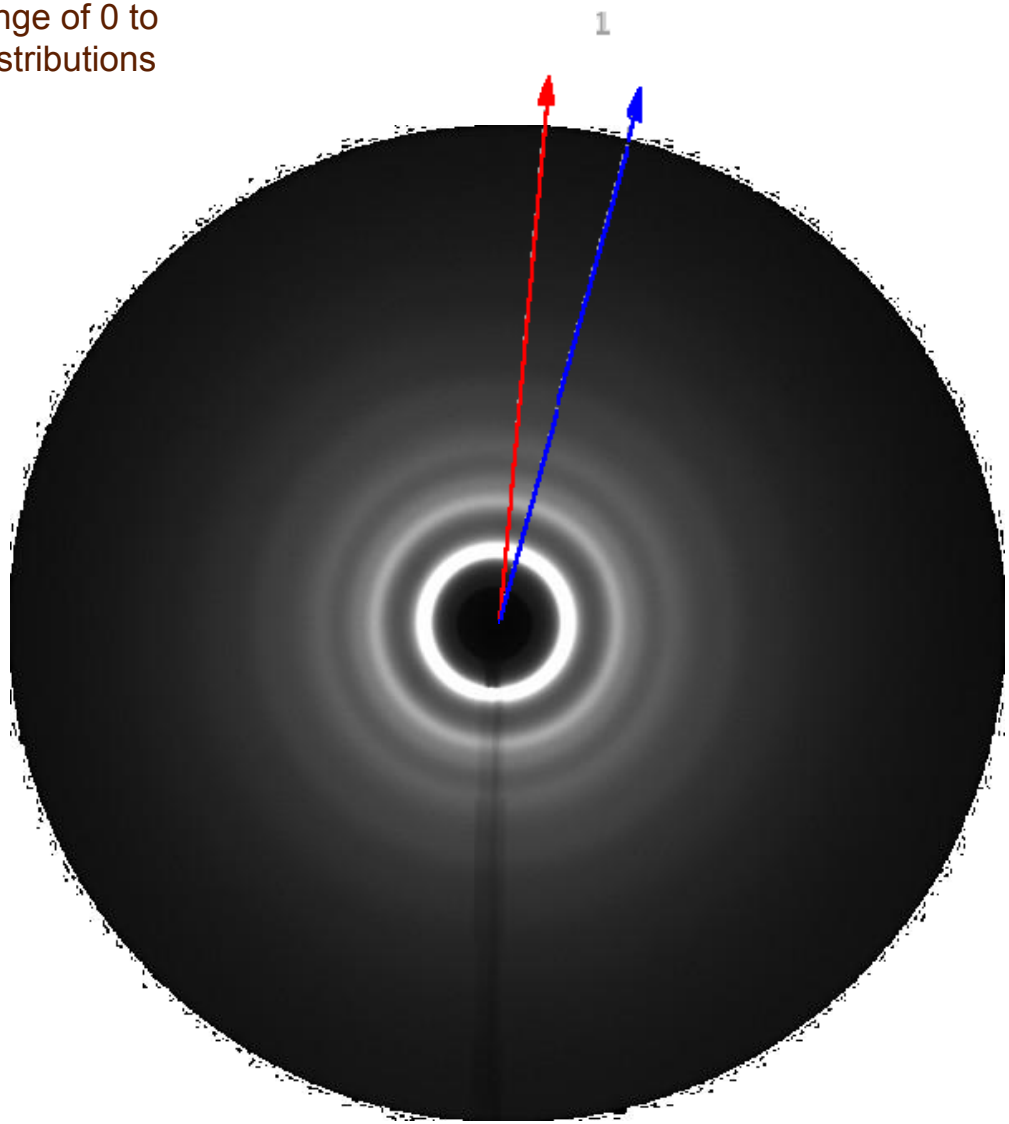

Determination of tensor components

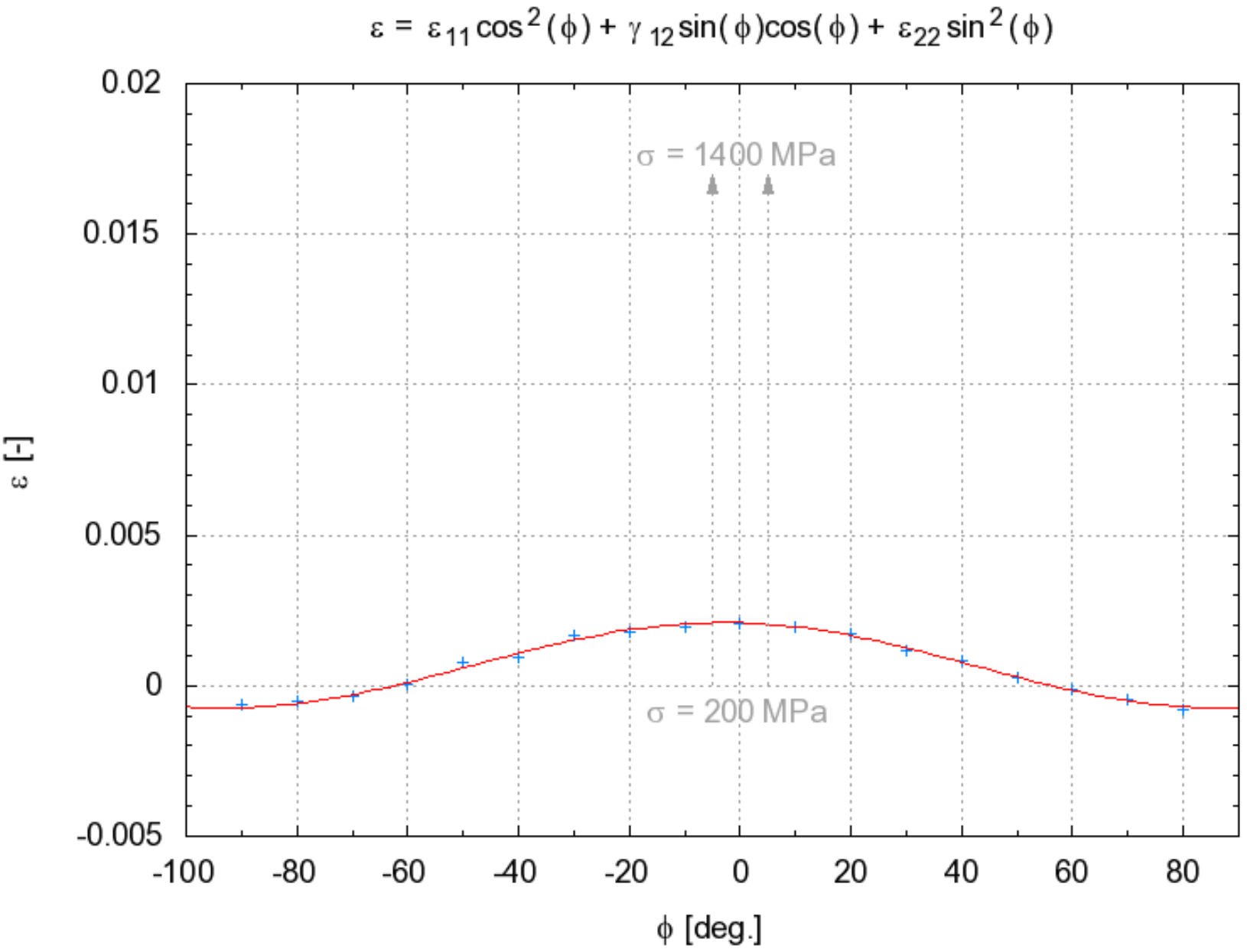

Analysis in reciprocal space

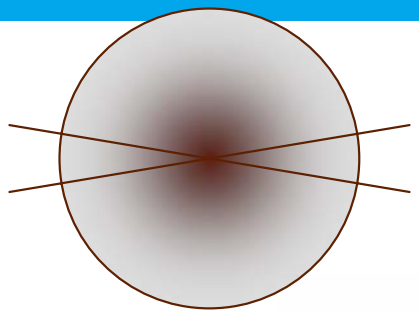

$$S(Q) = 1 + \frac{I_e(Q) - \left[\sum_{i=1}^{n} c_i f_i^2(Q)\right]}{\left[\sum_{i=1}^{n} c_i f_i(Q)\right]^2}$$

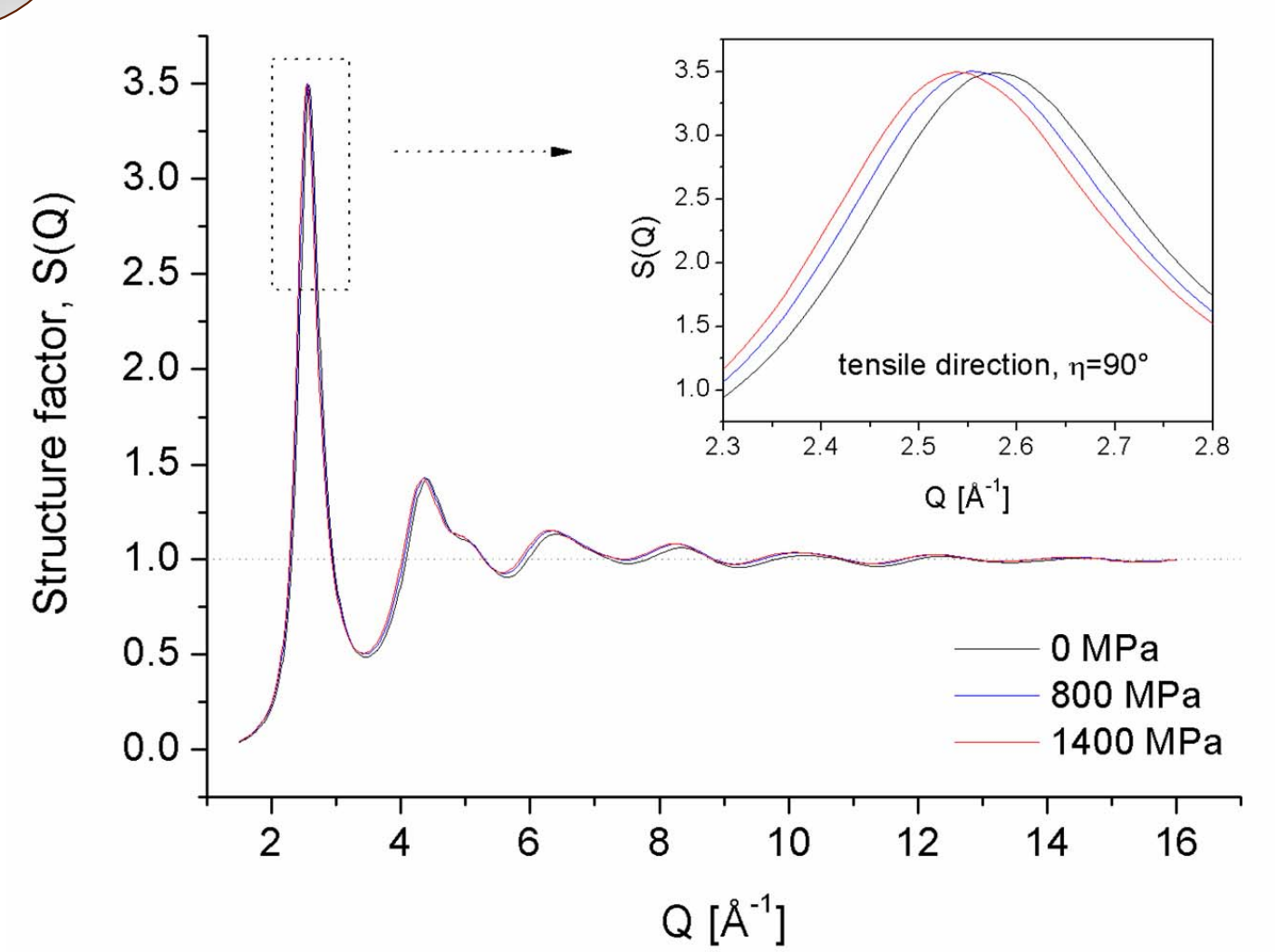

Stress-strain curves

Crystalline metal

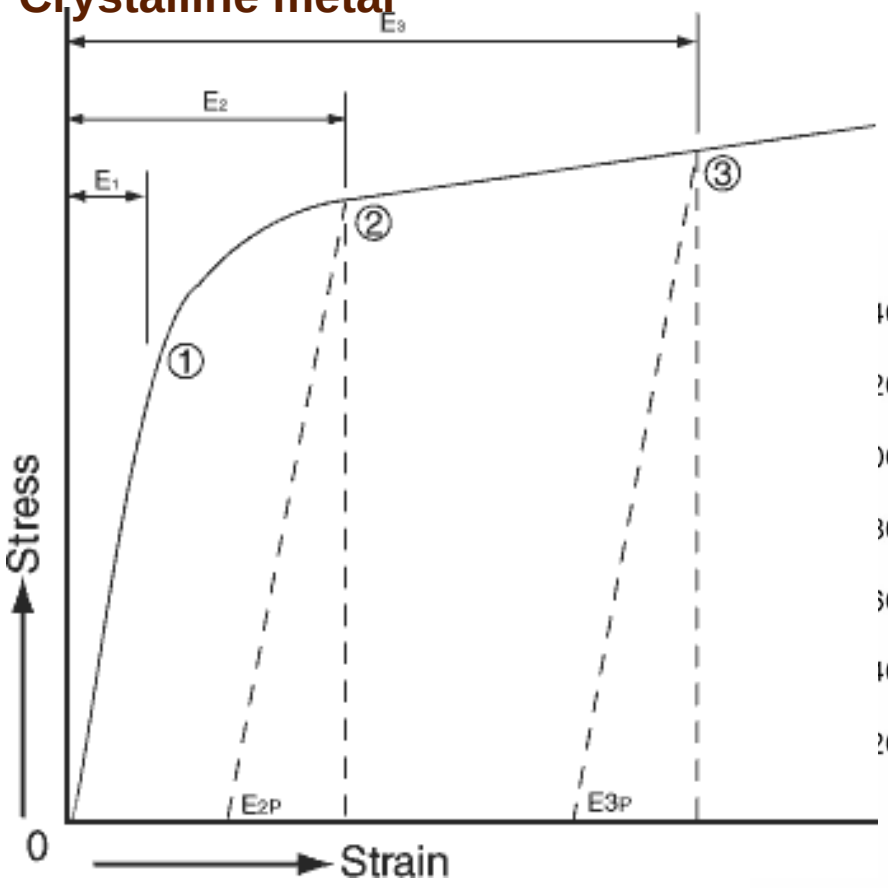

La based metallic glass

Only elastic strain !!!

Catastrophic failure !!!!

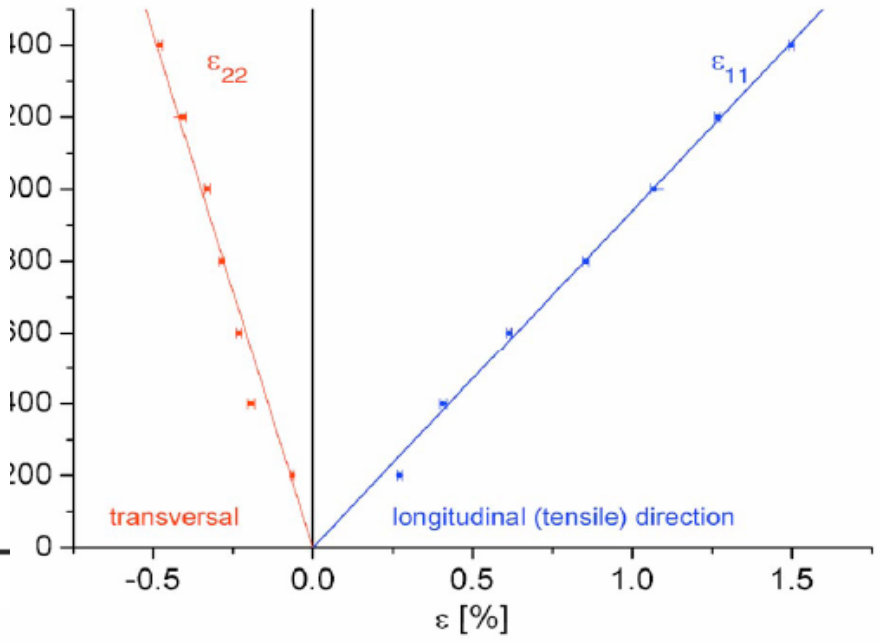

X.D. Wang et al 2009

Plastic deformation at high temperature

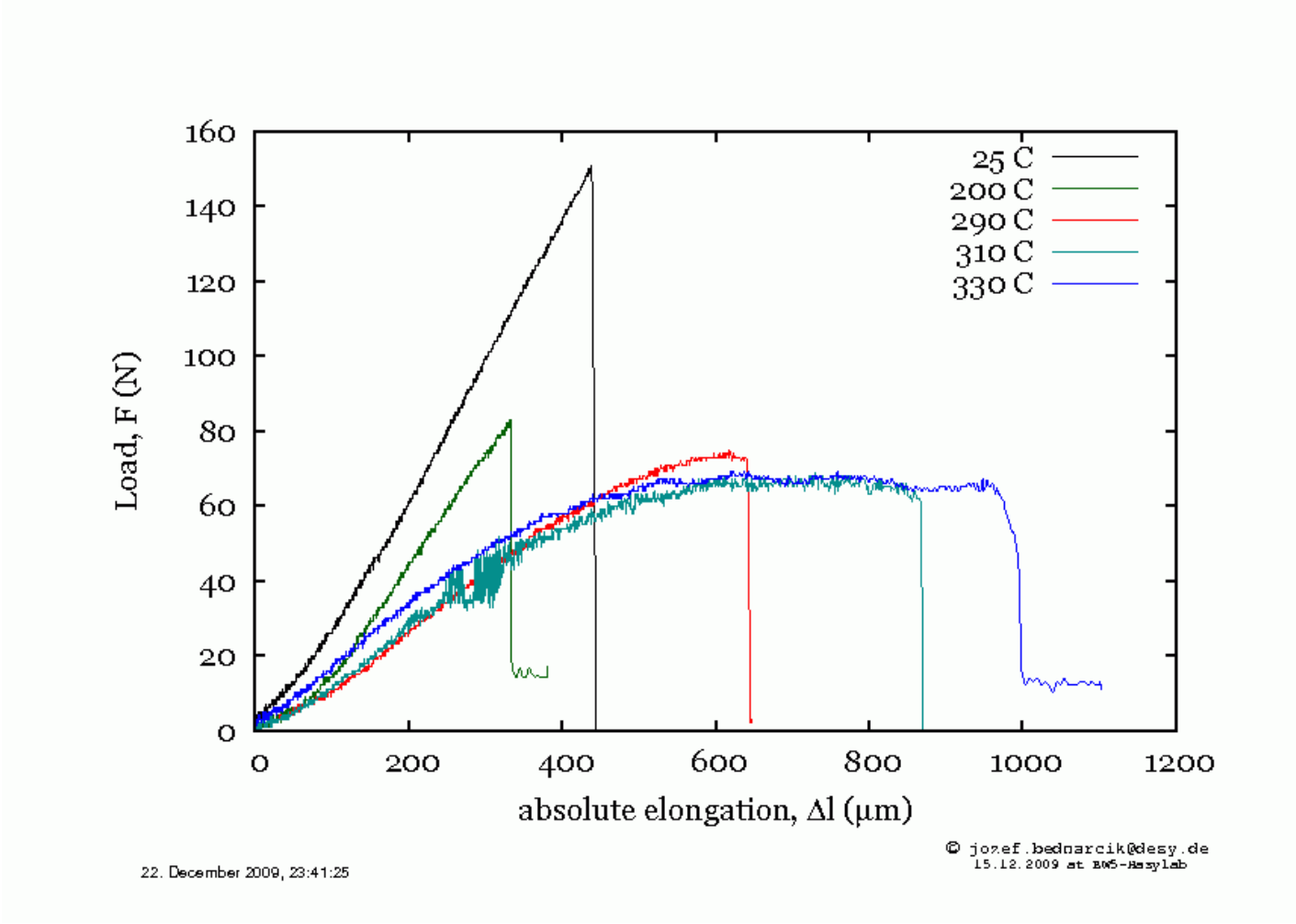

J. Bednarcik et al 2010

Summary

- Nuclear resonant scattering opens a time window to study the glass transition at the timescale of the α-relaxation around the critical point
- Confined systems can be selectively studied without background from the martix
- Bulk metallic glasses may be used as a simple model system to study glass-physics
- In addition they show some interesting mechanical properties
- Detailed structure studies may help to understand the process of glass formation